WILEY

Identification of groundwater mean transit times of precipitation and riverbank infiltration by two-component lumped parameter models

Nguyen Le Duy[1,2] | Nguyen Viet Dung[1,2] | Ingo Heidbüchel[3] | Hanno Meyer[4] | Markus Weiler[5] | Bruno Merz[1,6] | Heiko Apel[1]

[1]Section Hydrology, GFZ German Research Centre for Geosciences, Potsdam, Germany

[2]SIWRR Southern Institute of Water Resources Research, Ho Chi Minh City, Vietnam

[3]Department of Hydrogeology, Helmholtz Centre for Environmental Research GmbH–UFZ, Leipzig, Germany

[4]Research Unit Potsdam, Alfred Wegener Institute for Polar and Marine Research, Potsdam, Germany

[5]Faculty of Environment and Natural Resources, University of Freiburg, Freiburg, Germany

[6]Institute for Environmental Sciences and Geography, University of Potsdam, Potsdam, Germany

Correspondence
Nguyen Le Duy, Section Hydrology, GFZ German Research Centre for Geosciences, Potsdam, Germany.
Email: duy@gfz-potsdam.de

Abstract

Groundwater transit time is an essential hydrologic metric for groundwater resources management. However, especially in tropical environments, studies on the transit time distribution (TTD) of groundwater infiltration and its corresponding mean transit time (mTT) have been extremely limited due to data sparsity. In this study, we primarily use stable isotopes to examine the TTDs and their mTTs of both vertical and horizontal infiltration at a riverbank infiltration area in the Vietnamese Mekong Delta (VMD), representative of the tropical climate in Asian monsoon regions.

Precipitation, river water, groundwater, and local ponding surface water were sampled for 3 to 9 years and analysed for stable isotopes ($\delta^{18}O$ and δ^2H), providing a unique data set of stable isotope records for a tropical region. We quantified the contribution that the two sources contributed to the local shallow groundwater by a novel concept of two-component lumped parameter models (LPMs) that are solved using $\delta^{18}O$ records.

The study illustrates that two-component LPMs, in conjunction with hydrological and isotopic measurements, are able to identify subsurface flow conditions and water mixing at riverbank infiltration systems. However, the predictive skill and the reliability of the models decrease for locations farther from the river, where recharge by precipitation dominates, and a low-permeable aquitard layer above the highly permeable aquifer is present. This specific setting impairs the identifiability of model parameters. For river infiltration, short mTTs (<40 weeks) were determined for sites closer to the river (<200 m), whereas for the precipitation infiltration, the mTTs were longer (>80 weeks) and independent of the distance to the river.

The results not only enhance the understanding of the groundwater recharge dynamics in the VMD but also suggest that the highly complex mechanisms of surface–groundwater interaction can be conceptualized by exploiting two-component LPMs in general. The model concept could thus be a powerful tool for better understanding both the hydrological functioning of mixing processes and the movement of different water components in riverbank infiltration systems.

1 | INTRODUCTION

Environmental isotopes have been used commonly to identify the dynamics of groundwater systems. Environmental isotope techniques can provide insights into the origin of water (Maloszewski, 2000), the interaction between surface and groundwater (e.g., Stichler, Maloszewski, Bertleff, & Watzel, 2008; Stichler, Maloszewski, & Moser, 1986), subsurface flow conditions (K. McGuire, DeWalle, & Gburek, 2002), fundamental mixing processes (M. Stewart & Thomas, 2008), water transport (e.g., Maloszewski, Stichler, Zuber, & Rank, 2002; Kabeya, Katsuyama, Kawasaki, Ohte, & Sugimoto, 2007; M. K. Stewart, Mehlhorn, & Elliott, 2007), and recharge mechanisms (Koeniger, Gaj, Beyer, & Himmelsbach, 2016) in the subsurface system. Given that the hydraulic properties of aquifers are poorly known and spatially variable, environmental tracer methods can provide more accurate groundwater flow velocities and recharge rates than traditional hydraulic methods (Cook & Böhlke, 2000). For example, numerical flow models can overestimate or underestimate the flow velocity depending on the aquifer thickness, the hydraulic conductivity, and the effective porosity (Zuber, Różański, Kania, & Purtschert, 2011).

The groundwater transit time is an essential hydrologic metric that integrates the variety of subsurface flow paths, storage capacities, and mixing processes in the groundwater system. The mean transit time (mTT) describes the average time that water particles spend travelling through a system (K. J. McGuire & McDonnell, 2006), and the transit time distribution (TTD) describes the whole spectrum of transit times of those water particles transported through the system (Maloszewski, 2000). Knowledge of the TTD and its corresponding mTT is essential for groundwater resources management, for example, when installing groundwater extraction systems for water supply (Hiscock & Grischek, 2002), calibrating numerical groundwater transport models (Bethke & Johnson, 2008), evaluating the security of drinking water supplies (e.g., Darling, Morris, Stuart, & Gooddy, 2005; Eberts, Böhlke, Kauffman, & Jurgens, 2012), or understanding the sources of contamination (e.g., Morgenstern et al., 2015).

Most mTT estimation methods are based on the lumped parameter model (LPM), pioneered by Małoszewski and Zuber (1982). The LPM does not require detailed hydrological information and thus can be used for initial investigations of little known systems (Mook & Rozanski, 2000) where data are insufficient, for example, in developing countries or ungauged basins (K. J. McGuire & McDonnell, 2006). It is based on a lumped convolution integral (a black box model), in which an input signal is related to a specific transfer function (or a TTD) to obtain an appropriate output signal. A common assumption for the application of LPM is the time invariance of TTDs (see

Maloszewski & Zuber, 1996; K. J. McGuire & McDonnell, 2006). Assuming steady-state conditions, LPMs can be set up to determine the best-fit TTD and mTT for the best representation of the local subsurface flow conditions (Maloszewski & Zuber, 1996). In reality, however, many systems are dynamic and stationary conditions hardly ever met (Rinaldo et al., 2011). LPMs can be applied in a moving-window approach (e.g., Hrachowitz et al., 2009) to estimate the time-variant transit times and examine the nonstationary of TTDs (e.g., Hrachowitz, Soulsby, Tetzlaff, Malcolm, & Schoups, 2010; Heidbüchel, Troch, Lyon, & Weiler, 2012; Tetzlaff, Birkel, Dick, Geris, & Soulsby, 2014; Christian Birkel et al., 2016).

Despite the long history and high potential of hydrological applications (Leibundgut, Maloszewski, & Külls, 2011), studies on mTT in tropical environments are still rare (Christian Birkel et al., 2016; Mosquera et al., 2016), mainly due to financial constraints and data sparsity (zzzzBonell & Bruijnzeel, 2005). Moreover, most of these studies have focused on water transit times in African (e.g., Jacobs et al., 2018), Australian (e.g., Duvert, Stewart, Cendón, & Raiber, 2016; Lamontagne et al., 2015), and/or Central and Latin American regions (e.g., Roa-García & Weiler, 2010; Muñoz-Villers & McDonnell, 2012; Timbe et al., 2014; Farrick & Branfireun, 2015; Timbe et al., 2015; Christian Birkel et al., 2016; Mosquera et al., 2016; Muñoz-Villers, Geissert, Holwerda, & McDonnell, 2016). To our best knowledge, groundwater transit times from stable isotopes have never been quantified in Asian monsoon regions.

Groundwater modelling in the Vietnamese Mekong Delta (VMD) was pioneered by Haskoning B.V., DWRPIS (Boehmer, 2000) who set up a regional groundwater model. The author pointed out that groundwater recharge in most of the delta ranges from 0.01 to 1 mm/day and is dominated by (a) infiltration of precipitation and irrigation water, (b) downward leakage through the semipermeable layers of the Holocene aquifer, and (c) seepage from rivers, streams, and lakes. The water balance analysis suggested that recharge from rainfall and irrigation is significant (for the Plain of Reeds, see Figure 1) and slightly (for the whole VMD) smaller than that from the Mekong river branches and the canal system. Also, the hydraulic connection between shallow and deep groundwater is insignificant, except for the dune area along the coast of the eastern VMD (Boehmer, 2000).

Although groundwater has been determined to be closely linked to surface water in the Mekong floodplains (Kazama, Hagiwara, Ranjan, & Sawamoto, 2007; Raksmey, Jinno, & Tsutsumi, 2009) or significantly controlled by rivers and tributaries (Wagner, Tran, & Renaud, 2012), groundwater modelling is still challenging due to the sparsity of groundwater data (Johnston & Kummu, 2012). Recent modelling studies have focused on understanding groundwater dynamics (Nam, Goto, & Osawa, 2017; Nuber, Van Nam, & Stolpe,
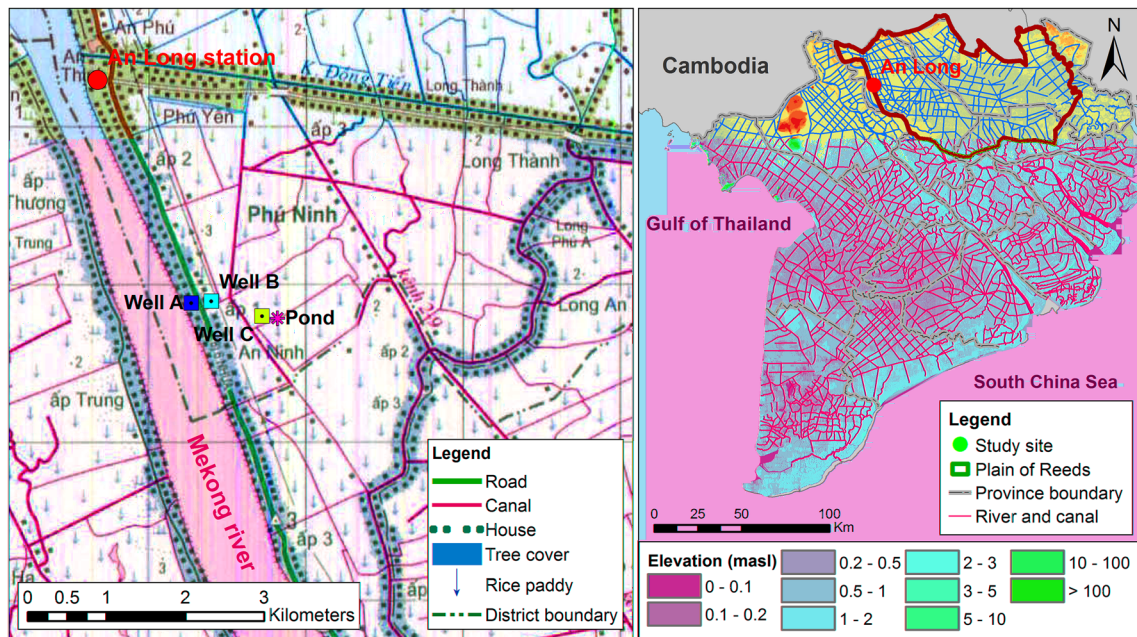
FIGURE 1 The Plain of Reeds in the Vietnamese Mekong Delta (right) and the study site (zoomed in) of An Long (left). The screening depths of Wells A, B, and C are 15, 12, and 14 m, respectively. The distance from Wells A, B, and C to the Mekong river is 140, 190, and 660 m, respectively. The pond with an area of approximately 500 m^2 and a depth of 2 m is used for fish farming. The distances from the pond to Well C and the Mekong river are around 40 and 700 m, respectively

2009; Vermeulen et al., 2013) and on evaluating land subsidence (Minderhoud et al., 2017). Despite the high demand on groundwater resources (Wagner et al., 2012) for household and industrial consumption (Danh & Khai, 2015), surface–groundwater interaction and groundwater recharge have not been sufficiently quantified (Thu, 2017). Instead, there has been considerable interest in the arsenic contamination of groundwater (Buschmann et al., 2008; Erban, Gorelick, Zebker, & Fendorf, 2013; Kocar et al., 2008; Merola, Hien, Quyen, & Vengosh, 2015; Shinkai, Truc, Sumi, Canh, & Kumagai, 2007; Stanger, Truong, Ngoc, Luyen, & Thanh, 2005) and general groundwater quality (An, Tsujimura, Phu, Ha, & Hai, 2018; Hoang, Bang, Kim, Nguyen, & Dang, 2010; Le Luu, 2017; Wilbers, Sebesvari, & Renaud, 2014) in the VMD. Also, tracer-based groundwater studies have primarily focused on qualitative aspects such as tracing the groundwater recharge sources (e.g., An et al., 2018; An, Tsujimura, Le Phu, Kawachi, & Ha, 2014; Ho et al., 1991; Thu, 2017). In other parts of the Mekong Delta, groundwater studies estimated the sources of recharge affected by evaporation, for example, from the wetland and ponds to the shallow groundwater in Cambodia (e.g., Lawson et al., 2013; Lawson, Polya, Boyce, Bryant, & Ballentine, 2016; Richards et al., 2018).

In this study, we primarily used stable isotope (δ^{18}O) time series to identify the mTTs of shallow groundwater and the optimized TTDs best describing the subsurface flow conditions when applying the two-component LPMs. The Plain of Reeds, serving as the seepage area for groundwater infiltration in the north-west region of the VMD (Boehmer, 2000), was chosen as a pilot area. For the sampling campaigns, the study site An Long in the Plain of Reeds (Figure 1) was selected, primarily considering logistic constraints. Although this area

may not be representative for the entire Mekong Delta, the site is likely indicative of the general nature of the near-stream subsurface flow dynamics because of the low variation of lithology and topography (Nguyen, Ta, & Tateishi, 2000) throughout the region. The information on subsurface mixing processes, the preferred flow pathways, and the transit times of water infiltration at riverbank areas resulting from long-term isotopic records could enhance the understanding of the groundwater dynamics as well as groundwater vulnerabilities in the VMD.

The general objective of this work was to test the applicability of two-component LPMs to examine TTDs and their mTTs in a riverbank infiltration system where two distinct water components are present. Our specific objectives were to (a) identify the dominant TTDs that best describe the subsurface flow conditions, (b) quantify the subsurface mixing processes and the time-variant mTTs of water near the riverbank, and (c) determine the uncertainty associated with parameter identification and model performance.

2 | STUDY AREA

The study area is located in the Plain of Reeds, in the VMD between latitudes 10°42′7″N to 10°48′9″N and longitudes 105°22′45″E to 105°33′54″E (Figure 1). The average elevation ranges from 1 to 4 m above sea level. The average annual rainfall is 1,400–2,200 mm, characterized by a distinct seasonal distribution (GSO, 2016; Renaud & Kuenzer, 2012). The annual average temperature is 27°C with monthly averages ranging from 25°C to 29°C. The annual average relative humidity ranges from 77% to 88%. The monthly evaporation

rate ranges from 67 to 80 mm and 76 to 109 mm in the rainy and dry season, respectively (GSO, 2016; Renaud & Kuenzer, 2012).

The hydrogeological units in the VMD are classified according to their geological formation: the Holocene, the Pleistocene, the Pliocene, and the Miocene aquifer systems. At the study site, the target aquifer is the Holocene sediment sequence. It is characterized by the uppermost layer of silt and clay (low-permeable aquitard), overlying a layer of fine to coarse sands (high-permeable aquifer). The average depths of aquitard and aquifer are approximately less than 11 m and 30 m below ground level, respectively (Minderhoud et al., 2017; Wagner et al., 2012). The grain sizes defined for clay, silt, fine and coarse sand, and fine gravel are 1–4 μm, 4–63 μm, 63 μm–2 mm, and 2–8 mm, respectively (Wentworth, 1922). The hydraulic conductivities of aquitard and aquifer are 0.02–0.2 m/day (for silt and clay) and 12–200 m/day (for fine to coarse sands), respectively (Boehmer, 2000). The effective porosities of clay and sand layers are 0.5 and 0.2, respectively (Benner et al., 2008).

3 | METHODS

3.1 | Water sampling and isotopic analysis

Precipitation and river water were sampled at An Long station. Groundwater was sampled at three wells (A, B, C) closed to the An Long station and the Mekong river (Figure 1). The distances from Wells A, B, and C to the Mekong river are 140, 190, and 660 m, respectively. The screening depths of these wells are 15, 12, and 14 m, respectively. These wells are used for household water supply only. Following the classification of aquifer systems by Wagner et al. (2012), the groundwater samples were collected from the Holocene aquifer and representative of the shallow groundwater in the VMD. A pond, located 700 m away from the Mekong river and used for fish farming, was included to provide information about the isotopic fractionation of local surface water by evaporation, characteristic for the floodplains during the monsoonal floods. The total number of samples and the schedule of water sampling are summarized in Table 1.

To avoid evaporation effects, we stored the collected samples in 30-ml plastic sample bottles with tight screw caps and kept all

TABLE 1 Water sampling at An Long

	Period	Frequency	Number of samples
Precipitation	06.2014–06.2015	Weekly	155
	06.2015–07.2017	Subweekly	
River water	01.2009–05.2010	Fortnightly	737
	06.2010–07.2017	Subweekly	
Well A	06.2014–07.2017	Weekly	157
Well B	06.2014–07.2017	Weekly	157
Well C	06.2014–07.2017	Weekly	157
Pond water	03.2016–12.2016	Weekly	42

samples in the dark before the laboratory analysis. The stable isotope samples were analysed at the Alfred-Wegener-Institute (AWI) in Potsdam, Germany. The measurements were performed with a Finnigan MAT Delta-S mass spectrometer using equilibration techniques to determine the ratio of stable oxygen ($^{18}O/^{16}O$) and hydrogen ($^2H/^1H$) isotopes. Analytical results were reported as δ^2H and $\delta^{18}O$ (‰, relative to Vienna Standard Mean Ocean Water) with internal 1σ errors of less than 0.8‰ for δ^2H and 0.1‰ for $\delta^{18}O$. The detailed measuring procedure is described in Meyer, Schönicke, Wand, Hubberten, and Friedrichsen (2000).

3.2 | Hydrological measurements

Groundwater and river water levels were recorded every 15 min between June 2015 and July 2017 by pressure sensors (HOBO U20 Fresh Water Level Data Logger). River water levels were monitored at An Long station, about 2 km upstream of the wells. Groundwater levels were observed at two additional monitoring wells screened at a depth of 15 m below ground level, in order to avoid disturbance of the level records by water extraction. The first monitoring well was installed between Wells A and B, and another one was located between Well C and the pond (Figure 1). The distance from the first and second monitoring wells to Wells A and C are 20 and 25 m, respectively. Sediment samples taken during the installation of these monitoring wells indicated that the upper aquitard layer (from 8 to 10 m below ground level) is dominated by clay and silty clay, whereas the aquifer layer below consists mainly of coarse sand. A terrestrial survey was carried out in June 2016 to reference all recorded water level measurements to the gauge at An Long, a national water level monitoring station. All water levels are reported as meters above sea level.

3.3 | Two-component LPMs

LPMs are based on the lumped convolution integral approach (Małoszewski & Zuber, 1982) to transform the tracer input signal (C_{in}) into the tracer output signal (C_{out}), considering a distribution of transit times according to a transfer function. M. K. Stewart and McDonnell (1991) introduced a more robust approximation by adding flow weights (w) to the isotopic composition of the input so that the outflow composition reflects the mass flux of tracer leaving the system (K. J. McGuire & McDonnell, 2006)

$$C_{out}(t) = \frac{\int_0^\infty C_{in}(t-\tau)w(t-\tau)g(\tau)d\tau}{\int_0^\infty w(t-\tau)g(\tau)d\tau}, \qquad (1)$$

where τ is the transit time, t is the time of exit from the system, and ($t - \tau$) represents the time of entry into the system; C_{in} and C_{out} are the input and output tracer signature, respectively; and $g(\tau)$ is the transfer function representing the assumed TTD of the subsurface flow system. This modification is more flexible than other recharge adjustment techniques (e.g., Grabczak, Różański,

Maloszewski, & Zuber, 1984; Maloszewski & Zuber, 1996) as the weighting term $w(t)$ can include any appropriate factor such as rainfall rates, throughfall rates, or effective rainfall (K. J. McGuire & McDonnell, 2006).

The recharge sources of shallow groundwater in the VMD are mainly river water and precipitation (Boehmer, 2000; Ho et al., 1991; Wagner et al., 2012). The output isotopic composition ($\delta^{18}O$) thus stems from the water of two different sources with likely different transit times. Therefore, the two-component LPMs were chosen for transit time modelling. We excluded a deep groundwater component because the connection between shallow and deep groundwater is insignificant (An et al., 2014; Boehmer, 2000; Ho et al., 1991). During the calibration, integrated parameters were adjusted to fit the measured isotopic records for each investigated well, following Weiler, McGlynn, McGuire, and McDonnell (2003). The model was rewritten in a modified two-component convolution equation:

$$C_{Well}(t) = p\frac{\int_0^\infty C_{inR}(t-\tau)w_R(t-\tau)g_R(\tau)d\tau}{\int_0^\infty w_R(t-\tau)g_R(\tau)d\tau} + (1-p)\frac{\int_0^\infty C_{inP}(t-\tau)w_P(t-\tau)g_P(\tau)d\tau}{\int_0^\infty w_P(t-\tau)g_P(\tau)d\tau},$$

(2)

where C_{inR} and C_{inP} are the input tracer signature of the river and precipitation infiltration, respectively; C_{Well} is the output tracer signature of an investigated well; $g_R(\tau)$ and $g_P(\tau)$ are TTD functions of the river and precipitation infiltration, respectively; p and $(1-p)$ are the fractions of the river and precipitation infiltration in the investigated well, respectively; and the weighting terms w_R and w_P are defined as follows:

$$w_{Ri} = \frac{N\alpha_i^R Q_i}{\sum_{i=1}^N \alpha_i^R Q_i},$$

(3)

$$w_{Pi} = \frac{N\alpha_i^P P_i}{\sum_{i=1}^N \alpha_i^P P_i},$$

(4)

where

1 N is number of measurements; Q_i is river discharge (m^3/s); and P_i is rainfall amount at An Long station (mm);

2 river infiltration coefficient: $\alpha^R = 1$ and $\alpha^R = 0$ for periods when the river water level is higher (losing streams) and lower (gaining streams) than the groundwater level, respectively. In this sense, $\alpha^R = 1$ (or $\alpha^R = 0$) indicates mass flux (or no mass flux) of tracer infiltrated from the river to a well;

3 precipitation infiltration coefficient: $\alpha^P = 1$ for months with precipitation infiltration (months in the rainy season) and $\alpha^P = 0$ for months without precipitation infiltration (dry season). We assumed that rainfall infiltrating to the shallow groundwater in the dry season is not significant due to the thickness (~9 m) of the upper low-

permeable aquitard (see Section 2) and the small rainfall amount during the dry season.

The fractions of the river (p) and precipitation ($1-p$) infiltration in each well can be derived by a linear mixing equation using long-term averages:

$$p = \frac{\bar{C}_{well} - \bar{C}_{inP}}{\bar{C}_{inR} - \bar{C}_{inP}},$$

(5)

where $\bar{C}_{well}$ is the mean $\delta^{18}O$ value of the investigated well and $\bar{C}_{inR}$ and $\bar{C}_{inP}$ are the weighted mean $\delta^{18}O$ values of river and precipitation infiltration (weighted by the weighting terms w_R and w_P, respectively).

3.4 | Selection and combination of TTDs

We tested six TTDs commonly applied in hydrologic systems: the exponential, linear, exponential-piston flow (EPF), linear-piston flow (LPF), advection–dispersion (AD, Maloszewski & Zuber, 1996; Cook & Böhlke, 2000), and the gamma model (Kirchner, Feng, & Neal, 2000). Although the EPF and AD models have been used in riverbank infiltration studies (e.g., Kármán, Maloszewski, Deák, Fórizs, & Szabó, 2014; Maloszewski, Rauert, Trimborn, Herrmann, & Rau, 1992; Stichler et al., 1986; Stichler et al., 2008) and in groundwater studies (e.g., Cartwright & Morgenstern, 2016; M. K. Stewart, Morgenstern, Gusyev, & Małoszewski, 2017), the exponential and gamma models have been widely applied for catchment mTT modelling (cf. K. J. McGuire & McDonnell, 2006; Hrachowitz et al., 2010).

Identifying TTDs that best describe the subsurface flow conditions requires both theoretical and experimental considerations (K. J. McGuire & McDonnell, 2006). Theoretically, the exponential distribution can only be applied for unconfined aquifers, whereas the combinations of exponential (or linear) and piston flow distributions or the AD distribution are more applicable for partly confined aquifers (Maloszewski & Zuber, 1996; Małoszewski & Zuber, 1982). Considering the hydrogeological setting of the Holocene aquifer, characterized by the upper low-permeable aquitard and the lower high-permeable aquifer, the exponential distribution (exhibiting flow lines with extremely short mTTs) seems therefore inappropriate for precipitation infiltration to wells screened at depth, but more adequate for riverbank infiltration to shallow groundwater (see Zuber et al., 2011). Hence, the optimization of two-component LPMs can be considered as an experimental approach to test the application of the selected TTDs.

Typically, each TTD function requires one or two fitting parameters. Table 2 summarizes the equations, the fitting parameters, and the predefined parameter ranges of TTDs used. The initial parameter ranges were assumed to be bounded, uniform distributions:

• The range of the mTT (τ_m) was limited to a maximum of 250 weeks, equivalent to approximately the maximum 5 years that mTTs can be determined using stable isotopes of water (Maloszewski &

TABLE 2 The TTD functions and their parameter ranges (assumed uniform distribution) for the GLUE analysis

Model	Transit time distribution $g(\tau)$	Parameter(s) range
Exponential distribution (E)	$\frac{1}{\tau_m} exp\left(\frac{-\tau}{\tau_m}\right)$	τ_m [1–250]
Linear distribution (L)	$\frac{1}{2\tau_m}$ for $\tau \leq 2\tau_m$ 0 for $\tau > 2\tau_m$	τ_m [1–250]
Exponential-piston flow distribution (EPF)	$\frac{\eta}{\tau_m} exp\left(-\frac{\eta\tau}{\tau_m} + \eta - 1\right)$ for $\tau \geq \tau_m\left(1 - \eta^{-1}\right)$ 0 for $\tau < \tau_m(1 - \eta^{-1})$	τ_m [1–250] η [1–4]
Linear-piston flow distribution (LPF)	$\frac{\eta}{2\tau_m}$ for $\tau_m - \frac{\tau_m}{\eta} \leq \tau \leq \tau_m + \frac{\tau_m}{\eta}$ 0 for other τ	τ_m [1–250] η [1–4]
Advection–dispersion distribution (AD)	$(4\pi P_D \tau/\tau_m)^{-\frac{1}{2}} \frac{1}{\tau} exp\left[-\frac{(1-\tau/\tau_m)^2}{4P_D \tau/\tau_m}\right]$	τ_m [1–250] P_D [0–1]
Gamma distribution (G)	$\frac{\tau^{\alpha-1}}{\beta^\alpha \Gamma(\alpha)} exp(-\tau/\beta)$	τ_m [1–250] α [0.001–10] $\beta = \tau_m/\alpha$

Abbreviations: P_D, dispersion parameter (dimensionless); α, shape parameter (dimensionless); β, scale parameter (dimensionless); Γ, gamma function; η, parameter indicating the contribution of each flow type (dimensionless), expressed as the total volume/volume with exponential (or linear) TTD; τ_m, subsurface mTT (weeks).

Zuber, 1996; K. J. McGuire & McDonnell, 2006; M. K. Stewart, Morgenstern, & McDonnell, 2010).

- The range of the parameter η was set to [1–4]. This parameter indicates the contribution of the different flow types, expressed as the ratio of the total volume to the volume with an exponential (or linear) distribution. When η is equal to 1, the mixed model becomes the pure exponential (or linear) model. When η approaches infinity, the mixed model is a close approximation of the well-known but unrealistic piston-flow model represented by a Dirac function. We limited the upper bound of η to 4 (equivalent to a maximum of 75% of piston flow in the TTD) to improve the convergence of the Monte Carlo simulations.

- The dispersion parameter (P_D) in the AD model should not exceed 2 for a constant tracer input (Maloszewski & Zuber, 1996). To improve the convergence of Monte Carlo simulations, we limited P_D to 1 (cf. Cartwright & Morgenstern, 2016), which is appropriate for kilometre-scale flow systems (Mook & Rozanski, 2000).

- The range of the shape parameter (α) in the gamma model was limited to 10, following Timbe et al. (2014) and M. K. Stewart et al. (2017).

To set up the two-component LPMs, the free combination of two TTDs (e.g., the exponential combined with the dispersion model) would yield a large number of possible set-ups. This approach would require a multitude of assumptions, increase computational cost, and model uncertainties. For computational reasons, as well as to keep the model as simple as possible, we assumed that the TTDs of precipitation and river infiltration are of the same type (e.g., exponential or linear piston-flow TTDs). The number of models to be tested is thus equal to the number of selected TTDs. Theoretically, unreasonable models, as for example, the double exponential model, which includes an exponential TTD for precipitation, are also included in order to test the theoretical limitations with observations in the model fitting. The hypothesis is that theoretically unreasonable models should be rejected during the model fitting.

3.5 | Model performance and uncertainty analysis

Monte Carlo experiments were used to find the best parameter sets. The generalized likelihood uncertainty estimation (GLUE) methodology (Beven & Binley, 1992) was applied to determine behavioural solutions (i.e., parameter sets giving acceptable predictions) and parameter identifiability. Due to the high number of fitting parameters, the analysis consisted of 10^6 iterations. For each model set-up, the model performance was evaluated using the Kling–Gupta efficiency (KGE; Gupta, Kling, Yilmaz, & Martinez, 2009) for describing the model performance and the root mean square error (RMSE) for describing the mass balance. Although the model performance based on KGE can be classified as good (KGE > 0.75), intermediate (0.75 > KGE > 0.5), weak (0.5 > KGE > 0), and very poor (KGE<0), following Thiemig, Rojas, Zambrano-Bigiarini, and De Roo (2013), there is no standard criterion to classify the performance based on RMSE. The model performance was therefore classified as satisfactory for KGE > 0.5. We finally used the solution with the Euclidean distance (D_E) between (1 − KGE) and RMSE as likelihood measures (see Equation (6)). The best 5% solutions in terms of D_E were selected as behavioural models, from which we constructed 90% confidence intervals of the estimated mTTs (see Mosquera et al., 2016; Timbe et al., 2014). We also examined the dotty plots to check that the selected solution provides a reasonably wide range of behavioural parameter set. In this study, $D_E = 1$ indicates a perfect fit.

$$D_E = 1 - \sqrt{(1 - KGE)^2 + (RMSE)^2}. \quad (6)$$

3.6 | Data preparation

Because data were collected at different temporal resolutions, from fortnightly to subweekly, all data were aggregated to weekly mean

values for consistency. The early fortnightly river water samples were repeated in order to obtain a weekly time series. This simplification does not affect the mTT analysis, as these data were used for model warm-up only. The actual model fitting was performed for the period of subweekly sampling of both river water and precipitation.

Considering the different length of the input time series (9 years of river water and 3 years of precipitation; cf. Table 1), the time series of precipitation was repeated back to January 2009 using monthly weighted means from the 3 years of available data. This procedure implies a stable inter-annual variation of precipitation isotopes, a reasonable assumption in the VMD (see Duy, Heidbüchel, Meyer, Merz, & Apel, 2018). The approach does not change the results of the mTT estimation while giving the models more room to find stable results (Hrachowitz, Soulsby, Tetzlaff, & Malcolm, 2011).

3.7 | Modification of the input function

The isotopic fractionation of precipitation before infiltration (e.g., due to evaporation or mixing processes) should be considered during the calibration of LPMs. Precipitation falling on the ground likely mixes with local surface water (e.g., ponds, rice paddies, and irrigated, inundated, or wetland areas) and partly evaporates before infiltrating. We considered the vertical infiltration as a mix of local surface waters and precipitation, both affected by evaporation. This assumption is in line with the suggestion that both river and evaporated-surface-water sources recharge groundwater along the Mekong river (Lawson et al., 2013; Lawson et al., 2016; Richards et al., 2018). Therefore, the input of precipitation infiltration was corrected, considering isotopic enrichment caused by evaporation.

We modified the input functions by adding a correction factor (Δ) to the isotopic composition of precipitation. This factor accounts for the isotopic enrichment due to the evaporation and mixing processes before the infiltration. This value was assumed to be constant and was derived by accounting for the potential evaporation in the region. However, in order to quantify the uncertainty that is introduced by a constant correction factor, a sensitivity analysis of the model results to the isotopic correction of precipitation infiltration was conducted (cf. Section 3.8). All modified input functions are referred to as precipitation infiltration. The input of river infiltration was not isotopically corrected, implying no isotopic fractionation before and during the infiltration process.

3.8 | Model set-up

In order to get deeper insights into the model behaviour, parameter identifiability, and uncertainties, three LPM set-ups were defined (Tests 1, 2, and 3). The uncertainties were attributed to errors

(1) the modified input functions (correction factor Δ),

(2) the mass balance analysis (value of p integrated into the two-component LPMs), and

(3) the assumed nonstationary or steady-state conditions during the calibration.

We assumed steady-state conditions to be dominant in the groundwater system and estimated time-invariant mTTs in Tests 1 and 2. For Test 3, the two-component LPMs were applied in a moving-window approach (e.g., Heidbüchel et al., 2012; Hrachowitz et al., 2009) to examine the time-variant TTDs and their corresponding mTTs. The detailed set-ups of these tests are as follows.

3.8.1 | Test 1: Modified input functions

We varied the correction values (Δ^{var}) in the range between 0‰ and 5‰ (with increments of 0.2) to create 26 modified input functions. $\Delta^{var} = 0$‰ indicates no isotopic enrichment, and $\Delta^{var} = 5$‰ (mean value + standard deviation) represents the likely maximum isotopic enrichment before infiltration. The upper limit is derived from the distribution of differences between isotopic content of rainfall and pond water. It represents the mean value + 1 standard deviation, that is, the 84% quantile. Because we could not use another tracer (e.g., Cl) to independently assess the uncertainties of the mass balance analysis, the fraction of river infiltration was considered a fitting parameter (p^{cal}) and calibrated accordingly. Depending on the assumed TTD function, three or five parameters were fitted during the calibration with each of the 26 modified input functions. In this test, 9-year records of $\delta^{18}O$ were used (the first 6 years for a warm-up and the last 3 years for analysis).

3.8.2 | Test 2: Mass balance

We fixed a correction value ($\Delta^{fix} = 1.81$‰), defined by the isotopic difference between the arithmetic mean value of the pond water and the weighted mean value of precipitation. The aim was to match the mean values of the modified input function and the pond water, implying that the precipitation ponding on the ground is mixed with preexisting local surface water and partly evaporates before infiltrating to the groundwater. In this test, the fraction of river infiltration was predefined by Equation (5) and used as a fixed parameter (p^{fix}). The motivation for this test was that the contribution of river (or precipitation) infiltration should be identical independent of the selected TTDs. This was tested with this approach. Consequently, two or four fitting parameters (depending on the assumed TTD) were fitted with the modified input function created by Δ^{fix}. Similar to Test 1, we used 9-year records of $\delta^{18}O$.

3.8.3 | Test 3: Nonstationarity

Nonstationarity is implicitly considered by the weighing according to discharge (Equation (3)) and the alpha coefficient determining the seasonal variation between losing and gaining stream conditions. However, possible additional nonstationarity caused by changes in the state of the surface–groundwater system was investigated. This was performed by a moving-window approach. Windows of 2-year length (adding previous 6 years for warm-up) were applied with a 2-week increment to create overall 29 sliding-window sequences of the

isotopic time series. The window length was defined sufficiently long to accommodate the identified mTTs in Tests 1 and 2, which vary up to almost 3 years (cf. Section 4.3). In this analysis, [Δ^{fix}, p^{fix}] were used to calibrate the two-component LPMs in order to avoid over-parametrization. For computational reasons, only the best-suited TTD identified in Tests 1 and 2 was used to estimate the time-variant mTTs. The Bayesian information criteria (BIC) was selected as a parsimoniousness metric (C. Birkel, Dunn, Tetzlaff, & Soulsby, 2010; Hrachowitz et al., 2010) to identify the best-suited TTD. A lower BIC value suggests a better model, considering the model performance in relation to the number of fitting parameters.

$$BIC = n \ln \left(\frac{SSE}{n} \right) + k \ln(n), \tag{7}$$

where n is the number of observations, k is the number of fitting parameters, and SSE is the sum of squared errors.

4 | RESULTS

4.1 | Surface–groundwater interaction

Considerable dynamics of surface–groundwater interaction were observed at the study site, as depicted by the similar water level variations up to 2 m annually in the river and groundwater (Figure 2). Seasonal changes in groundwater levels observed between Wells A and B mostly lay between those found in Well C and the river. The groundwater level observed at wells closer to the river (Wells A and B) exhibited a higher seasonal variation than the site farther from the river (Well C).

Gaining or losing stream conditions were defined as river water penetrating into the groundwater system or groundwater seeping out into the river, respectively (Fetter, 2001). Losing stream periods (higher monthly river water level than groundwater level) were detected mainly during the flood season from July to November, whereas gaining stream periods were observed primarily during the
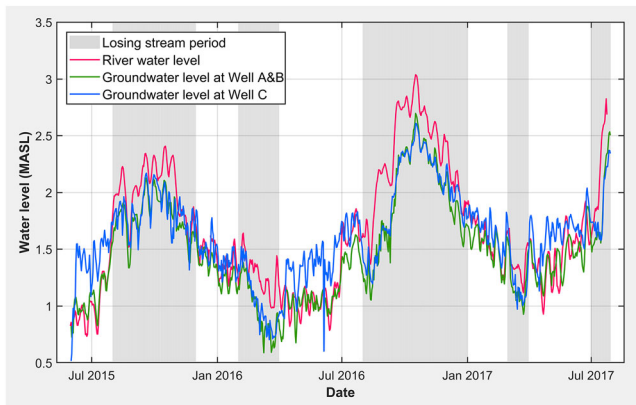
FIGURE 2 The daily groundwater and river water levels at An Long. Grey background indicates losing stream periods when the monthly river water level is higher than the monthly groundwater level

end of the dry season from April to June (Figure 2). From December to February, the differences between river water and groundwater levels were insignificant. These months were considered as the transition period between losing and gaining stream conditions.

4.2 | Stable isotope ratios

Figure 3 shows the isotopic data sets of precipitation, river, pond water, and groundwater on a dual-isotope plot of $\delta^{18}O$ and δ^2H. The isotopic compositions vary between the dry and rainy seasons with more negative values during the rainy seasons. The precipitation $\delta^{18}O$ ranges between −13.7‰ and −1.0‰, with an arithmetic mean value and a standard deviation of −6.0‰ ± 2.5‰. The precipitation δ^2H varies between −98.7‰ and 0.9‰, with a mean and standard deviation of −38.6‰ ± 19.3‰.

The isotopic composition of river water showed a variation from −9.6‰ to −5.3‰ and −70.3‰ to −40.2‰ for $\delta^{18}O$ and δ^2H, respectively. The arithmetic mean values and standard deviations for $\delta^{18}O$ and δ^2H were −7.6‰ ± 0.8‰ and −55.6‰ ± 5.9‰, respectively. The river samples plotted below the local meteoric water line (LMWL) and exhibited a regression line with a less steep slope than the LMWL.

The isotopic composition of pond water showed considerable variability ranging from −9.4‰ to 3.6‰ and −66.6‰ to 5.3‰ for $\delta^{18}O$ and δ^2H, respectively. The arithmetic mean values and standard deviations for $\delta^{18}O$ and δ^2H were −4.6‰ ± 3.0‰ and −37.3‰ ± 15.8‰, respectively. The pond water exhibited an evaporation trend with a slope of 5.3, suggesting that the isotopic enrichment is likely caused by evaporation taking place at 70–85% humidity (Clark & Fritz, 1997), comparable with the range of average annual relative humidity (77–88%) in the VMD.

All groundwater samples plot below the LMWL and are distinctly separated corresponding to the sampling wells. According to the distances from Wells A (140 m), B (190 m), and C (660 m) to the river, more negative isotopic values were observed at the wells located closer to the river. The arithmetic mean values (±standard deviation) for $\delta^{18}O$ of Wells A, B, and C were −6.1‰ ± 0.3‰, −5.5‰ ± 0.2‰, and −5.2‰ ± 0.6‰, respectively.

4.3 | Stationary transit time modelling

Figure 4 shows the results of Test 1 for the three investigated wells considering the sensitivity of model performances and parameter identifiability to the isotopic correction (based on the likelihood measure D_E). The model performances based on KGE and RMSE statistics are shown in Figure S1. The fitting accuracy generally increased with an increasing correction factor (Δ^{var}) up to 1.4‰, remained stable around the peak for Δ^{var} between 1.4‰ and 2.6‰, and decreased slightly after that. The best performances were identified for the LPF model (Figure 4d), followed by the AD model (Figure 4e). Notably, the optimum correction value (Δ^{var} = 1.8‰), providing the best LPF model performance, was very close to the isotopic difference between the
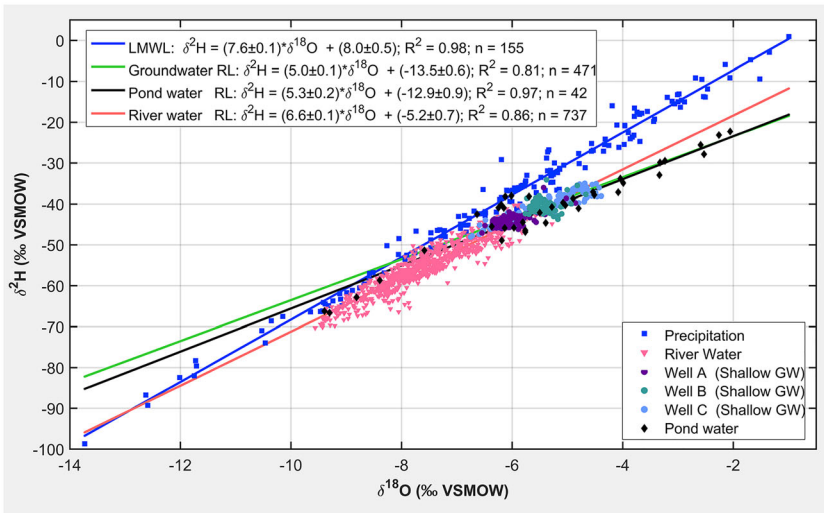
FIGURE 3 The isotopic data at An Long in a dual isotope plot. The regression line (RL) for groundwater is derived using all groundwater samples from all the wells. GW, groundwater; LMWL, local meteoric water line; VSMOW, Vienna Standard Mean Ocean Water
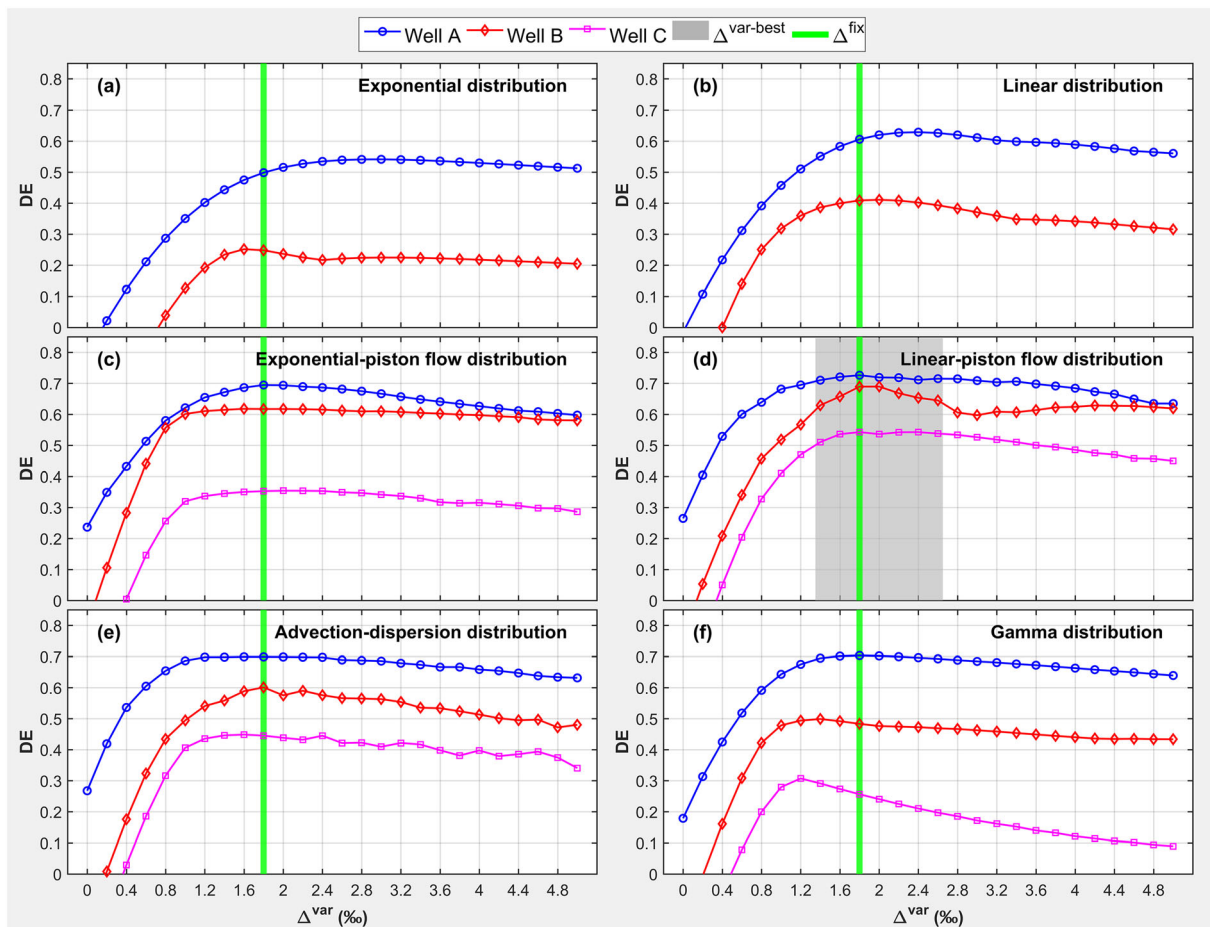
FIGURE 4 Sensitivity of the efficiency of two-component lumped parameter models to isotopic correction values (Δ^{var}) measured by using the Euclidean distance (D_E) between (1 – Kling–Gupta efficiency [KGE]) and root mean square error values. The green reference line indicates the isotopic difference (Δ^{fix}) between the arithmetic mean value of the pond water and the weighted mean value of precipitation. $\Delta^{var-best}$ corresponds to the best-possible model performance and reasonable parameter identifiability (see Figure 5). Negative likelihood measures ($D_E <$ 0) are not shown

arithmetic mean value of the pond water and the weighted mean value of precipitation (Δ^{fix} = 1.81‰). This supports the validity of the assumed fixed correction factor.

To evaluate the sensitivity of the parameter identifiability to the isotopic input correction, we focused on the LPF models providing the best-fit accuracies. The behavioural solutions (90%
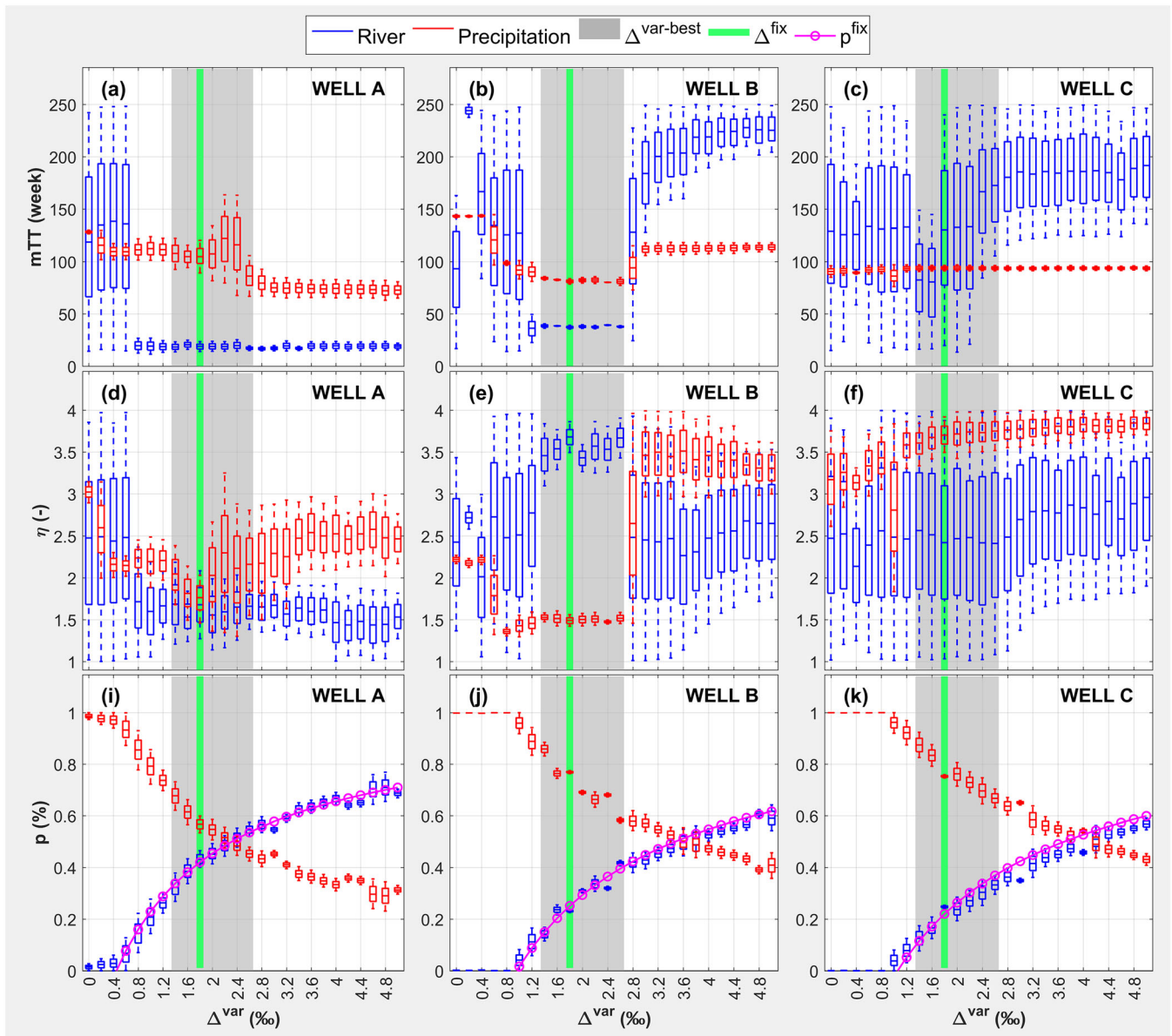
FIGURE 5 Sensitivity of the parameter identifiability of the linear piston flow model (i.e., the best-performing model) to the correction values (Δ^{var}) for all tested wells. The box plots indicate the 90% confidence intervals of fitting parameters given by the generalized likelihood uncertainty estimation analysis. Each box shows the interquartile range, the whiskers show the minimum and maximum values associated to 1.5 times the interquartile range. p (calibrated parameter) and p^{fix} (predefined by Equation (5)) are the fractions of recharge from river (or precipitation) infiltration; mTT is the tracer's mean transit time; η is a parameter indicating the ratio of total volume/volume with linear transit time distribution. $\Delta^{var\text{-}best}$ indicates the range for reasonable parameter identifiability. The explanation of Δ^{fix} is similar to Figure 4

confidence bound of the GLUE analysis) corresponding to a threshold of 5% of the best predictions by LPF models are shown in Figure 5. For other TTDs, results of optimized behavioural solutions are shown in Figure S2a–e.

Isotopic correction factors between 1.4‰ and 2.6‰ ($\Delta^{var\text{-}best}$ in Figures 4d and 5a–c) provided both acceptable fitting accuracies ($D_E >$ 0.5) and reasonable identifiability of mTTs. Therefore, only the estimated mTTs obtained with these correction factors were considered for further analysis and discussion below.

Considering each investigated well, the estimations of river mTTs were identical for the identified range of acceptable isotopic corrections (Figure 5a–c, blue boxes in the grey-shaded areas). Shorter mTTs of river infiltration were determined consistently for sites closer to the river. The optimized river mTTs ranged approximately from 15 to 20 weeks for Well A, from 35 to 40 weeks for Well B, and from 25 to 240 weeks for Well C. The parameter identifiability of river mTTs was better for the sites close to the river (e.g., Wells A and B).

The behavioural solutions of precipitation mTTs were identical for Wells B and C, independent of the isotopic correction and the distance of wells to the river. For Well A, the behavioural mTTs were also very similar, with a tendency to a larger range for higher acceptable correction factors. Compared with riverbank infiltration, the precipitation infiltration exhibited longer mTTs. Optimized precipitation mTTs were between 75 and 110 weeks with low uncertainties for all tested sites (Figure 5a–c). However, the LPF model provided poor constraints of parameter η, indicating different ratios of linear or piston flows at different investigated sites (Figure 5d–f). The uncertainty bounds of river infiltration fraction (p^{cal}) were quite narrow and increased with higher Δ^{var} (Figure 5i–k). Analogously, the fraction of precipitation infiltration ($1 - p^{cal}$) decreased with higher Δ^{var}.

Results in Test 2 were compared with the best-fit results in Test 1 (e.g., using $\Delta^{var} = 1.8‰$), considering the model efficiency (Figure 6), the fractions of water components contributing to the shallow groundwater (Figure 5 i–k), and the behavioural solutions of optimized mTTs (Figure 7). The best-fit results (LPF models) of the tests are reported in Table 3. The model performances (corresponding to the best-matching likelihood measures) of these tests were comparable (Figure 6a,b,d,e) and relatively good (>0.7) in terms of the KGE statistic for all investigated wells. Although the model parsimoniousness is slightly better within the set-ups in Test 2, illustrated by lower BIC values (see Figure 6c,f and Table 3), the dotty plots indicate that the

parameter identifiability of two of these tests is comparable (see Figures S3 and S4). Better parameter identifiability of river mTTs is observed for sites close to the river (e.g., Well A). Conversely, parameter identifiability of precipitation mTTs is much better for sites farther from the river (e.g., Well C).

4.4 | Identification of best-suited TTD

Out of all 18 models (three tested sites and six models per site), the threshold of model acceptance (KGE > 0.5) was fulfilled in 13 cases (Figure 6a,d). The five poor models with KGE < 0.5 were the exponential (E), the linear (L), and the gamma (G) models at two sites located farther from the river (Wells B and C). The EPF, the LPF, and the AD models provided satisfactory performances for all sites. Unsurprisingly, the more complex models (EPF, LPF, AD, and G) performed better than the simpler models (E and L), depicted by higher KGE and lower RMSE values. However, a better fit obtained with a higher number of adjustable parameters does not necessarily mean that an adequate model was found. Based on the model selection criterion (the lowest BIC), the best performing model type for all sites was the LPF model (Figure 6c, f). The other goodness-of-fit measures (KGE and RMSE; Figure 6a, b,d,e) confirmed this ranking. Although the LPF model can better constrain the behavioural solutions of optimized mTTs (Figure 7),
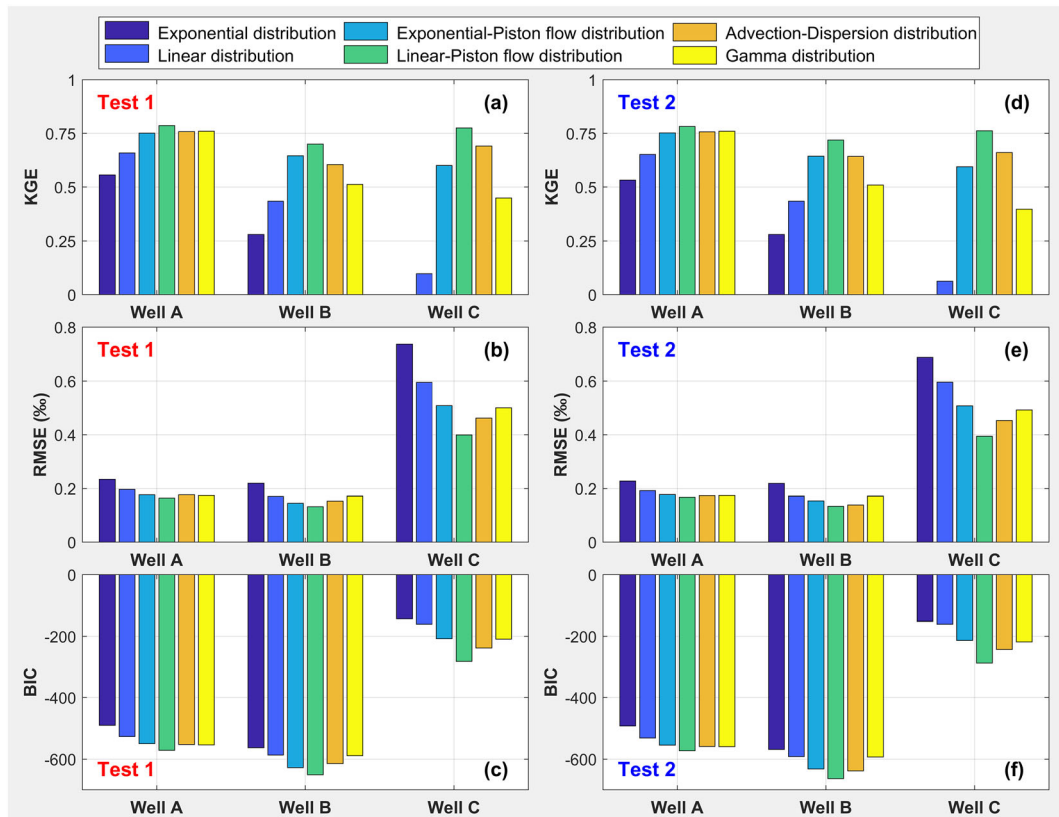
FIGURE 6 Comparison of Tests 1 (left) and 2 (right) for model efficiencies (the best performing models according to best likelihood measures). The two-component lumped parameter models were calibrated with [Δ^{var}, p^{cal}] and [Δ^{fix}, p^{fix}] for Tests 1 and 2, respectively. Negative Kling–Gupta efficiency (KGEs) are not shown. RMSE, root mean square error; BIC, Bayesian information criteria
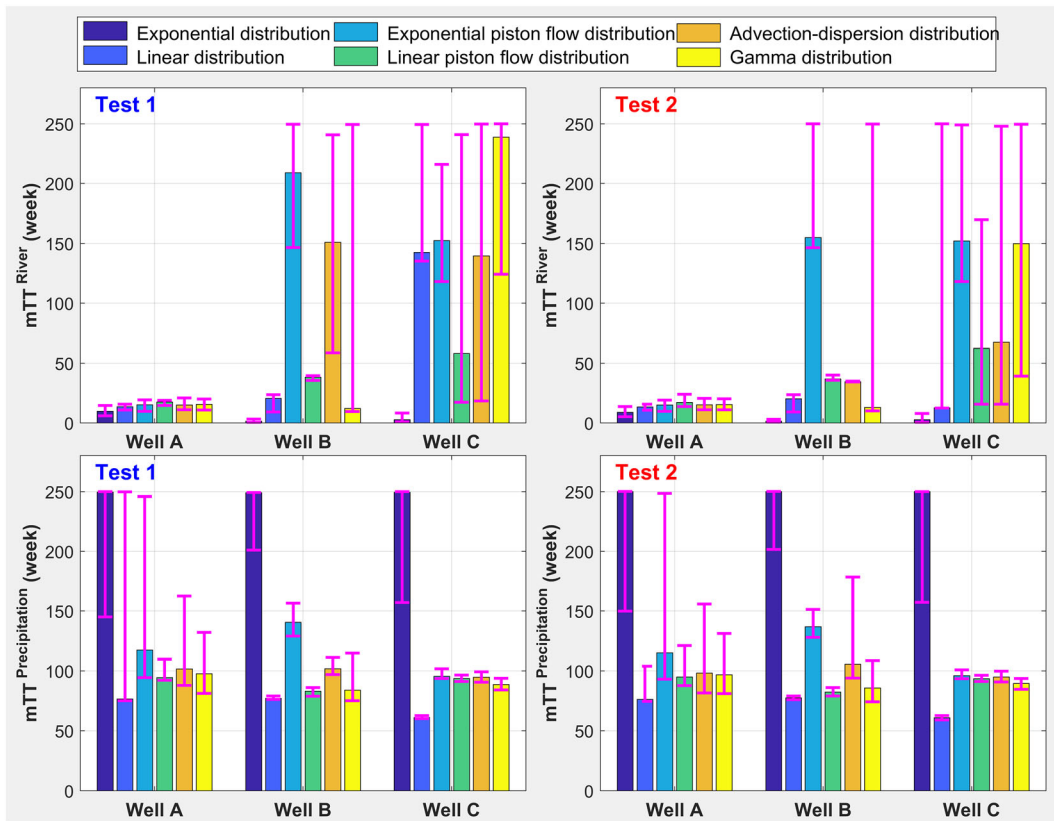
FIGURE 7 Estimated mean transit times (mTTs) of river (top) and precipitation (bottom) infiltration in Tests 1 (left) and 2 (right). The error bars indicate the 90% confidence intervals of mTT given by the generalized likelihood uncertainty estimation analysis

the dotty plots illustrate comparable parameter identifiability for all tested models (see Figure S4). Figure 8 shows the best-fit modelled $\delta^{18}O$ of LPF models and the uncertainty interval (90 % confidence bound of the GLUE analysis).

4.5 | Time-variant transit time modelling

Following the identification of the best-suited TTD, we calibrated the LPF model within the moving-window approach (Test 3) to estimate time-variant mTTs. The 2-year moving window with 2-week increments resulted in 29 best-fit LPF models for the study period from June 2014 to July 2017. Figure 9 shows varying model performance, a wide range of mTTs, and their associated parameter uncertainties (90% confidence limits) derived from the GLUE analysis. For all 29 models, the goodness of fit measured by the KGE statistic was reasonable (>0.5), suggesting reliable estima-tions of time-variant mTTs.

Considering each investigated well, the best-fit mTTs of river infil-tration were identical (stable in time) with acceptable parameter uncertainties (Figure 9). The best-fit mTTs of river infiltration were approximately between 16 and 24 weeks for Well A, between 36 and 48 weeks for Well B, and between 17 and 55 weeks for Well C. The uncertainties of river mTT were better constrained for sites close to the river. Regarding precipitation infiltration, the best-fit mTTs were

relatively similar (mainly around between 85 and 125 weeks) for all investigated wells. However, the uncertainties of precipitation mTTs were poorly constrained for the Well A close to the river compared with Well C farther from the river. In general, the uncertainty of river mTTs increased with distance to the river, whereas the uncertainties for precipitation infiltration mTTs decreased with distance to the river. Also, stationary and time-variant mTTs estimated by LPF models were comparable, in terms of both best-fit and behavioural solutions (Table 3).

5 | DISCUSSION

5.1 | Mechanisms and sources of groundwater recharge

Similar seasonal fluctuations between groundwater and river levels over the monitoring period (Figure 2) suggested a good hydraulic con-nection between surface water and groundwater along the Mekong river. The semi-annual reversal of gradients between the river and the groundwater indicates groundwater recharge, that is, that the river loses water to bank infiltration and recharges the Holocene aquifer during flooding. In contrast, groundwater is released from the aquifer to compensate for the small amount of river water at the end of the dry season. Considering the difference of the hydraulic conductivity

TABLE 3 Statistical parameters of the observed and simulated $\delta^{18}O$ time series by LPF models for Wells A, B, and C within the three model set-ups (Tests 1, 2, 3)

Test case	Observed Mean ± σ (‰)	Simulated Mean ± σ (‰)	Bias (‰)	KGE (-)	RMSE (‰)	BIC	Parameter	Units	River Best-fit	River Behavioural solution Low	Up	Precipitation Best-fit	Precipitation Behavioural solution Low	Up
Well A														
Test 1	−6.07 ± 0.26	−6.07 ± 0.25	0.004	0.79	0.16	−572	τ_m	Week	17.5	14.5	18.8	94.4	92.1	109.9
							η	(-)	1.83	1.36	1.98	1.86	1.62	1.95
							p	%	41.9	37.9	46.0	58.1	54.0	62.1
Test 2	−6.07 ± 0.26	−6.08 ± 0.25	0.010	0.78	0.17	−573	τ_m	Week	17.1	13.6	23.9	95.0	87.6	121.3
							η	(-)	1.82	1.26	2.07	1.90	1.40	2.03
							p	%	42.1			57.9		
Test 3[a]	−6.10 ± 0.23	−6.10 ± 0.22	0.00	0.74	0.16	−392	τ_m	week	18.2	15.6	22.3	107.0	83.9	135.9
							η	(-)	1.71	1.28	1.91	1.98	1.39	2.60
							p	%	43.2			56.8		
Well B														
Test 1	−5.45 ± 0.18	−5.46 ± 0.17	0.01	0.70	0.13	−651	τ_m	Week	38.3	35.3	39.5	83.0	78.8	86.1
							η	(-)	3.44	3.44	3.88	1.55	1.45	1.56
							p	%	24.7	21.0	27.8	75.3	79.0	72.2
Test 2	−5.45 ± 0.18	−5.47 ± 0.18	0.02	0.72	0.13	−664	τ_m	Week	36.8	35.5	40.0	82.3	78.9	85.9
							η	(-)	3.77	3.26	3.78	1.52	1.42	1.61
							p	%	25.1			74.9		
Test 3[a]	−5.47 ± 0.15	−5.48 ± 0.15	0.01	0.72	0.12	−472	τ_m	Week	41.4	32.9	67.4	88.1	80.4	96.6
							η	(-)	2.97	1.97	3.73	1.68	1.44	1.87
							p	%	25.7			74.3		
Well C														
Test 1	−5.25 ± 0.63	−5.22 ± 0.58	−0.03	0.78	0.40	−282	τ_m	Week	58.0	17.2	240.7	93.7	91.0	96.4
							η	(-)	2.90	1.06	3.91	3.75	3.50	3.96
							p	%	20.0	24.7	26.0	80.0	75.3	74.0
Test 2	−5.25 ± 0.63	−5.27 ± 0.57	0.02	0.76	0.39	−287	τ_m	Week	62.3	15.5	169.8	93.5	91.1	96.4
							η	(-)	3.62	1.00	4.00	3.75	3.49	4.00
							p	%	22.0			78.0		
Test 3[a]	−5.43 ± 0.65	−5.59 ± 0.59	0.17	0.72	0.47	−162	τ_m	Week	38.3	27.0	57.0	93.7	91.1	96.2
							η	(-)	2.86	1.41	3.81	3.78	3.46	3.97
							p	%	27.1			72.9		

Abbreviations: BIC, Bayesian information criteria; KGE, Kling–Gupta efficiency; p, fraction of recharge from river (or precipitation) infiltration; RMSE, root mean square error; σ, standard deviation; η, parameter indicating the ratio of total volume/volume with exponential (or linear) TTD; τ_m, tracer's mTT; (-), dimensionless.

Note. The simulated results and model efficiencies are presented for the best-matching likelihood measures (D_E). The model set-ups (including modified input functions, calibrated parameters, and assumed conditions) of these tests are described in Section 3.8.

[a]Mean values of the 29 best-fit LPF models are reported.

and the elevation of the aquitard and aquifer layers, the shallow groundwater is mainly in horizontal hydraulic contact with the river via bank infiltration at the highly permeable aquifer (characterized by the medium and coarse sand layer), instead of the low-permeable aquitard (characterized by the silt and clay layers).

Compared with precipitation and river water, groundwater showed strong damping of the isotopic signals, reflecting water storage systems dominated by subsurface flow paths (Dunn et al., 2008) with relatively long transit times (Hrachowitz, Savenije, Bogaard, Tetzlaff, & Soulsby, 2013). The unique stepwise increase in heavy

FIGURE 8 The observed and modelled δ¹⁸O plotted with the behavioural solutions (90% confidence bound of generalized likelihood uncertainty estimation analysis) corresponding to a threshold of 5% of the best prediction by the linear-piston flow models. Error bars indicate the analytical reproducibility of the δ¹⁸O measurements. VSMOW, Vienna Standard Mean Ocean Water
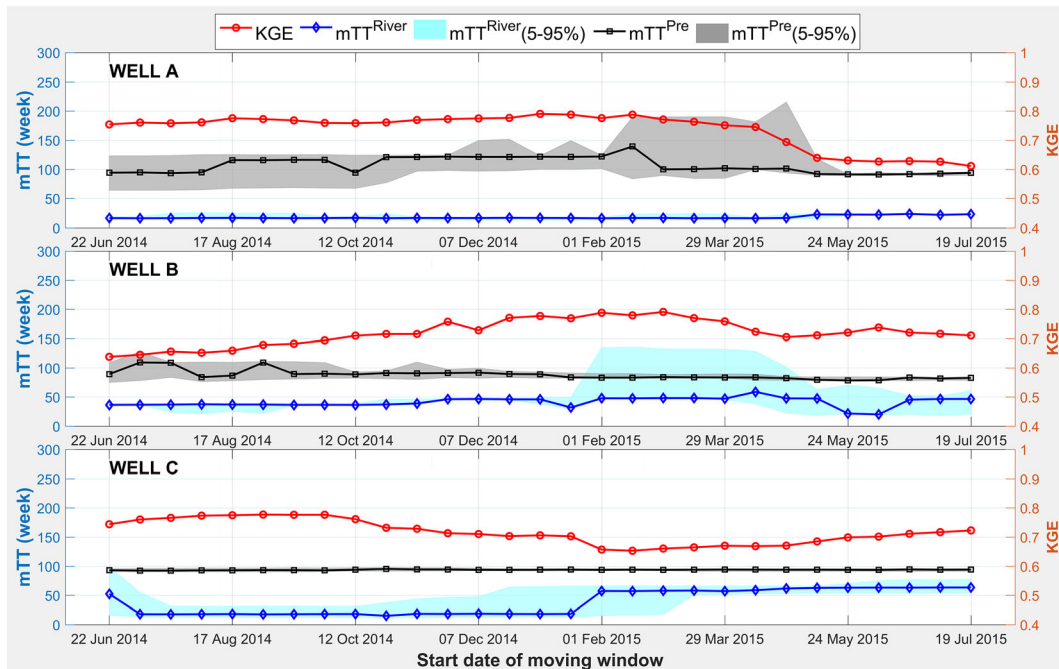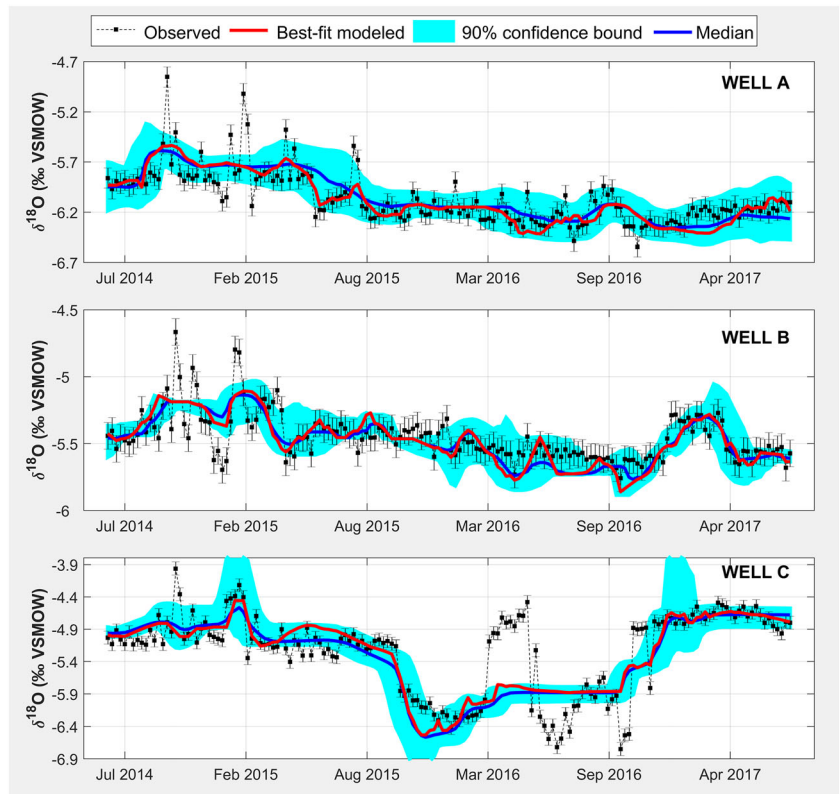
FIGURE 9 Model efficiencies (Kling–Gupta efficiency [KGE]) and the mean transit times (mTTs) of river and precipitation infiltration corresponding to the best-matching linear-piston flow models. The shaded areas represent the best behavioural solutions (90% confidence) of mTT predictions by generalized likelihood uncertainty estimation analysis. Results of time-variant mTTs are shown for every 2 weeks

isotopes observed in the groundwater with increasing distance from the river (Figure 3) might be explained by the mixing of riverbank infiltration with a more significant contribution from an evaporated

recharge source to the shallow groundwater. The isotopic signatures indicate the different importance of the two sources for the groundwater recharge at the investigated sites, as one would also expect

from a hydraulic point of view due to the different distances to the river. With increasing distance, the exchange between groundwater and river is usually dampened due to infiltration length and associated longer transit times.

The groundwater regression line deviated significantly from the LMWL exhibiting a less steep slope, whereas it compared well with the regression line of the pond water (Figure 3). This indicates that the local surface water, being affected by evaporative fractionation processes, is likely a second source recharging the shallow groundwater. The slopes derived from the regression lines of groundwater and pond water in our study are comparable with those in Lawson et al. (2013), Lawson et al. (2016), and Richards et al. (2018), who also suggested an evaporated source of surface recharge (e.g., from the wetland and ponds) to the groundwater in Cambodia. Such comparable results support the assumption that the precipitation is mixed with preexisting local surface water and evaporates before infiltrating down the unsaturated zone towards the shallow groundwater in the VMD. Considering the offset of isotopic samples of the river from the local precipitation (Figure 3), it is unlikely that the river was recharged by the local precipitation but is preferably sourced from upstream of the VMD (i.e., its run-off stems almost exclusively from the Mekong basin).

Generally, the analysis of water level fluctuations and isotopic signatures suggests that the shallow groundwater is recharged by two distinct water components via different flow pathways, justifying the use of two-component LPMs, beyond simple fitting considerations.

5.2 | Sensitivity of modelling results to isotopic correction

The sensitivity analysis (Test 1) illustrates that using modified input functions within the calibration of two-component LPMs can provide better fitting accuracies (Figure 4) without altering the estimated mTTs (Figure 5). Better performance was also reported when LPMs were calibrated with input functions modified by canopy interception (e.g., Stockinger et al., 2014), evapotranspiration (e.g., Stumpp, Stichler, & Maloszewski, 2009), or the correction of the isotopic mass balance (e.g., Viville, Ladouche, & Bariac, 2006). In this study, the correction was necessary because of (a) isotope enrichment in ponding water and (b) theoretical preconditions for the application of the mixing models, specifically the assumption that the water at the wells is the product of mixing of both river water and precipitation. Therefore, the $\delta^{18}O$ content of the well must range between the $\delta^{18}O$ content of the sources. This precondition is not fulfilled if the original $\delta^{18}O$ values of precipitation are used. Mass balance analysis indicates an unrealistic situation that there is no contribution of river infiltration to groundwater when the correction values are lower than 1.0‰ (Figure 5i–k) and, hence, justifies the isotopic correction. However, it has to be noted that the quantification of contributions from the two sources is sensitive to the isotopic correction of precipitation, depicted by the increase of p^{cal} with higher Δ^{var}.

A comparison between Tests 1 and 2 illustrates that the predefined mixing process (e.g., using Equation (5)) and fixed

correction for the $\delta^{18}O$ precipitation (e.g., Δ^{fix} = 1.81‰ to produce the same mean value of precipitation infiltration as the ponding water) provide reasonable modelling results. In this context, it is noteworthy that the best model results are obtained with Δ^{var} = 1.8‰, which is almost identical to Δ^{fix}. This similarity supports the validity of the definition of Δ^{fix} by the mean difference between precipitation and ponding water isotopic content. The fixing of the correction factor not only fulfils real-world and theoretical constraints but also improves the parsimoniousness of the applied model. A similar correction of $\delta^{18}O$ of precipitation (1.4‰) was applied by Calderon and Uhlenbrook (2016) for a hydrograph separation in Nicaragua, a climatic environment somewhat similar to this study.

5.3 | Dominant subsurface flow conditions

The relatively high performance (KGE > 0.7 and RMSE < 0.4‰, Table 3), better parsimoniousness (Figure 6c,f), reasonable parameter identifiability of mTT (Figure 7), and low fitting uncertainty (Figure 8) of the LPF model suggest that the LPF distribution likely represents the subsurface flow conditions at the study site. Other evidence supporting the dominance of linear and piston flow distributions and justifying the best performance of the LPF model are the poor performances of (a) the exponential model compared with the linear model and (b) the related non-linear models (EPF or gamma model) compared with the related linear models (e.g., LPF model; see Figure 6). This suggests that the subsurface transport of water is better characterized by a linear distribution rather than by an exponential distribution. This confirms that the exponential model is inadequate to represent recharge to groundwater collected at larger depths below the ground surface (Zuber et al., 2011). Secondly, mTT modelling results suggest a considerable fraction of piston flow in the TTDs. For example, considering the results of Test 2 from the LPF model for Well A (see Table 3), the best-fit value of η = 1.82 for river water implies that 55% of the volume of the river water infiltration passes through the aquifer as linear flow, whereas 45% can be characterized by piston flow behaviour. Accordingly, the value of η = 1.90 for precipitation implies a 53% of volume portion of linear flow and a 47% volume of piston flow in the TTD of precipitation infiltration.

The statistical findings indicate that the subsurface flow condition at the study site is likely best described with a linear distribution accounting for the infiltration along the river followed by the hydraulic replacement of groundwater caused by pressure gradients that adds the piston flow component to the model. The explanation is consistent with the hydrogeological setting at the study site characterized as a partially confined aquifer that does not create a phreatic system. This situation can be represented by a linear-piston model or a dispersion model according to the five hydrogeological settings described in Małoszewski and Zuber (1982). The accordance of the statistical finding with these theoretical considerations serves as a corroboration of the ranking of models (see Section 4.4) by the model fitting and the GLUE analysis.

Compared with the gamma model, the EPF and AD models provide better performances (Figure 6). The results agree well with the

dominance of these TTDs in riverbank infiltration studies (e.g., Kármán et al., 2014; Maloszewski et al., 1992; Stichler et al., 1986; Stichler et al., 2008) and/or in groundwater studies (e.g., Cartwright & Morgenstern, 2016; Stewart et al., 2017), whereas the gamma model has been frequently used in catchment studies (cf. K. J. McGuire & McDonnell, 2006; Hrachowitz et al., 2010). Although the LPF distribution has been introduced early (see Maloszewski & Zuber, 1996; Małoszewski & Zuber, 1982), it has rarely been tested, to our best knowledge, within the lumped parameter approach. Our study agrees well with Timbe et al. (2014), who suggested that the LPF model could be a reliable method to determine water transit times in southern Ecuador.

5.4 | Two-component LPM reveals recharge mechanism

Comparisons of the results (e.g., estimated mTT, parameter identifiability, and model efficiency) of three tests (Table 3) suggest that two-component LPMs can be applied to investigate mTTs and TTDs of different water components in tracer studies. We combine theoretical considerations and measurements of the hydrogeological setting with the best-fit LPF models (reported in Table 3) to develop a conceptual model of surface–groundwater interaction at the study site. The conceptual model (Figure 10) shows the spatial variation of mTTs, the different recharge contributions, and the subsurface flow conditions.

The contributions of the two recharge sources change with distance to the river. The mTTs of riverbank infiltration increase with the length of the horizontal flow path and the decreasing flow path

gradient between river and groundwater. The mTTs of river infiltration are relatively short (approximately 13–40 weeks) for locations close to the river (Wells A and B), but cannot be constrained for sites farther from the river (Well C). Notably, using stable isotopes alone cannot provide reliable longer mTTs, despite the used LPMs (Seeger & Weiler, 2014; Kirchner, 2016a), indicating the contribution of older water (>5 years) to the groundwater system of the VMD. The mTTs of precipitation infiltration were independent of the distance to the river, depicted by the relative similarity of mTTs (82–95 weeks) for all investigated wells. The fact that the estimated mTTs of precipitation infiltration are longer than the ones of river infiltration is attributable to the hydraulic conductivity of the soil. The horizontal infiltration from the river takes place mainly via the highly permeable aquifer, resulting in short mTTs (<40 weeks) for the investigated wells located close to the river (e.g., <200 m). Meanwhile, the vertical infiltration of precipitation (after ponding on the surface) takes place primarily via a low-permeable overlying aquitard, resulting in considerably longer mTTs (>80 weeks) for all investigated wells.

Overall, the results follow the general understanding of groundwater hydraulics and are reasonable from physical and hydrological points of view, corroborating the applicability of two-component LPMs to identify groundwater mTTs at riverbank infiltration systems. However, in the given lithological setting, the predictive skill and particularly the reliability of the models decrease for locations farther from the river, where recharge by precipitation dominates and a low-permeable aquitard layer above the aquifer is present. This specific setting impairs the identifiability of model parameters in this case. In other settings, for example, without an overlying aquitard, better model performance and parameter identifiability can be expected even for larger distances to the river.
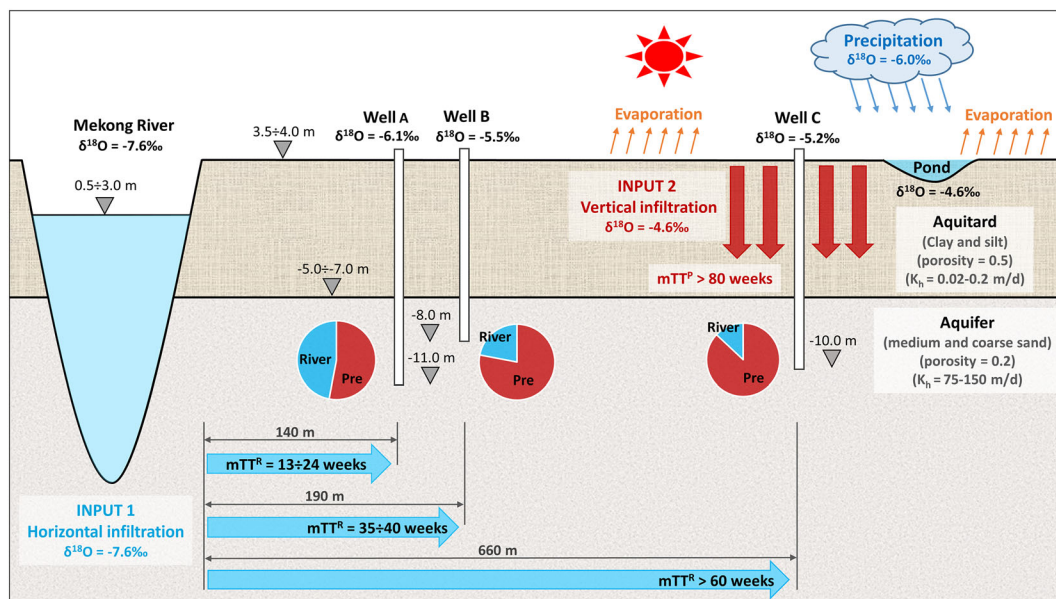
FIGURE 10 Conceptual model of subsurface flow conditions at the study site. The mean transit times (mTTs; arrows) and recharge contributions (pie charts) of river water and precipitation shown here result from the linear-piston flow model. The characteristics of the aquitard and aquifer layers (e.g., the thickness, type of soil, porosity, and vertical hydraulic conductivity) are referenced from (Benner et al., 2008; Boehmer, 2000; Minderhoud et al., 2017)

5.5 | Limitations and wider implications

Although the identified results are hydrologically plausible, corroborating the validity of the model concept, we acknowledge the limitations of this study. Here, we point out possible reasons related to the inevitable errors of two-component LPMs and shortcomings of data that could add uncertainties to the mTT analysis.

First, the lumped convolution modelling approaches rely on steady-state conditions and assumed nonstationary TTDs (Tests 1 and 2). Such assumptions are probably less problematic for groundwater than they are for surface water systems (Christian Birkel et al., 2016), yet they are rarely met in any real hydrologic setting (Rinaldo et al., 2011). Although time variance was introduced to the TTDs and their corresponding mTTs (Test 3), within each 2-year time frame of the moving window, steady-state conditions prevailed. The limitation of the time series by a moving window resulted in a somewhat poorer description of the groundwater system because the moving window was hardly larger than the mTT of precipitation infiltration. Consequently, our results concerning time-variable TTDs and mTTs should be considered a first step towards an analysis of nonstationary in surface-groundwater interaction.

Second, potential aggregation biases might lead to an underestimation of the mTTs in the heterogeneous system (see Kirchner, 2016b; Stewart et al., 2017). The mixing between vertical and horizontal recharge might not be correctly described with the LPMs; thus, the resulting mTTs could be biased by the selection of the method. To what extent this theoretical restriction applies to the presented results cannot, however, be determined.

Third, this work relying solely on stable isotopes cannot provide the ages of water older than 5 years (M. K. Stewart et al., 2010), which could result in the truncation of water transit time and skew the understanding of how the system stores and transmits water (M. Stewart, Morgenstern, McDonnell, & Pfister, 2012). Consequently, the identified mTTs should be considered partial transit times with preference for young waters contributing to shallow groundwater in the VMD. To evaluate potential contributions of older water fraction, environmental isotopes (e.g., tritium) have been frequently used (e.g., M. K. Stewart et al., 2010; Morgenstern et al., 2015; Cartwright & Morgenstern, 2016; Duvert et al., 2016).

Fourth, the study would have benefited from higher sampling frequencies (e.g., daily) to provide better insights into short-term system responses (see Hrachowitz et al., 2010; Christian Birkel et al., 2016). Higher sampling resolution could also improve model conceptualization and calibration (e.g., C. Birkel et al., 2010) and reduce potentially misleading insights (Hrachowitz et al., 2011) and uncertainties of mTT modelling (Timbe et al., 2015). However, given the practical constraints and costs of isotope sampling, higher sampling frequencies are difficult to realize in general.

Fifth, the reconstruction of the precipitation record (see Section 3.6) could be a potential source of error. However, the approach of looping precipitation isotopic signature has been common practice when input time series are too short to constrain mTT estimates adequately (e.g., Timbe et al., 2014; Christian Birkel et al., 2016; Mosquera et al., 2016; Muñoz-Villers et al., 2016). For more reliable palaeoclimate reconstructions of precipitation isotopes in Asian monsoon regions, model-based statistical approaches (e.g., the combination of global climate models with statistical analyses) could be applied (see Duy et al., 2018, and references therein).

Sixth, choosing the same types of TTDs to combine in the two-component LPMs cannot provide an entire picture of all possible combination of selected TTDs. Although mixing different kinds of TTDs (e.g., the combination of AD model for precipitation infiltration and LPF model for river infiltration) could improve the model performance, we expect that this approach invalidates the estimated mTTs, because most of the TTD types are relatively flexible and tend to accommodate themselves to the data. However, this approach should be considered in further study.

Finally, although the isotopic correction due to the evaporation process is in line with the hydrological setting (discussed in Section 3.7) and essential to fulfilling the theoretical constraints (discussed in Section 5.2), adding a constant value to the isotopic signature of rainfall to estimate the isotopic signature of vertical recharge unavoidably introduces uncertainties. This approach assumes a stable isotopic fractionation process for the whole study period, which is probably quite unrealistic. The sensitivity analysis revealed that although the mTTs are relatively insensitive to the correction factor, the identifiability of the contribution of the different sources to recharge is impaired by the correction factor. Moreover, if the water does pond on the surface before it infiltrates, the isotopic signature may be attenuated prior to recharge. This will result in mTTs being overestimated, because the presented approach does not account for the time required for evaporative changes in isotopic composition, but not for the time required for this. With the available data, it is impossible to analyse the isotopic enrichment of local surface water (e.g., Skrzypek et al., 2015) or independently assess actual contributions of infiltrated water components in this study. This could, for example, be achieved by using another tracer (e.g., Cl).

Despite these limitations, our results underline the usefulness of two-component LPMs in describing subsurface water movement at locations with different flow-path configurations and two groundwater recharge sources, for example, at riverbank infiltration areas. The concept could be further developed by utilizing two-component LPMs in conjunction with both stable and environmental isotopes (e.g., $\delta^{18}O$ and tritium). This could provide insights into the dynamics of both younger and older waters (e.g., <5 years and up to 200 years) contributing to the groundwater system. Generally, the model concept (integrating different TTDs of water components into LPMs) could be a powerful tool for better understanding the hydrological functioning of mixing processes and water movement in groundwater studies.

6 | CONCLUSIONS

This study investigated groundwater transit times and subsurface flow conditions at the riverbank infiltration areas in the VMD.

Precipitation, river, groundwater, and local surface water were sampled on a subweekly to weekly basis for different periods between 2009 and 2017 and analysed for stable isotopes. The applicability of two-component LPMs (allowing different TTDs for different recharge components) in conjunction with hydrological and isotopic measurements to identify subsurface flow conditions and the contribution to groundwater mixing was tested. The proposed method proved to be able to identify the TTDs and their corresponding mTTs of both river and precipitation infiltration to shallow groundwater using $\delta^{18}O$ records.

LPMs based on the LPF distribution were able to capture isotopic variations in shallow groundwater in response to the modified input function. Although the exact contribution of the water components infiltrating to the groundwater system remains uncertain, the dynamics of the surface–groundwater interaction could be identified. River water infiltrates horizontally mainly via the highly permeable aquifer, resulting in short mTTs (<40 weeks) for locations close to the river (<200 m). The vertical infiltration from precipitation takes place primarily via a low-permeable overlying aquitard, resulting in considerably longer mTTs (>80 weeks). The outcomes are hydrologically plausible, corroborating the validity of the applied approach. Our findings enhance the understanding of the shallow groundwater recharge dynamics and may serve as a baseline for future groundwater studies using environmental isotopes in the VMD. Groundwater resources management needs to consider the different recharge mechanisms and mTTs (mainly controlled by the distance to the river), resulting in different management options for different areas in the delta.

Our study suggests that the highly complex mechanism of surface–groundwater interaction and subsurface mixing processes at riverbank infiltration systems can be conceptualized by exploiting two-component LPMs. Regardless of the restrictions associated with certain errors of LPMs and the use of stable isotopes, the model concept can be transferred to other locations. Therefore the proposed model concept with the associated model selection procedure could provide a comprehensive hydrological tool for the analysis and understanding of groundwater recharge by different sources.

ORCID

Nguyen Le Duy https://orcid.org/0000-0002-3149-7473
Markus Weiler https://orcid.org/0000-0001-6245-6917
Bruno Merz https://orcid.org/0000-0002-5992-1440

REFERENCES

An, T. D., Tsujimura, M., Le Phu, V., Kawachi, A., & Ha, D. T. (2014). Chemical characteristics of surface water and groundwater in coastal watershed, Mekong Delta, Vietnam. *Procedia Environmental Sciences*, 20, 712–721. https://doi.org/10.1016/j.proenv.2014.03.085

An, T. D., Tsujimura, M., Phu, V. L., Ha, D. T., & Hai, N. V. (2018). *Isotopic and hydrogeochemical signatures in evaluating groundwater quality in the coastal area of the Mekong Delta*. Vietnam: Cham. https://doi.org/10.1007/978-3-319-68240-2_18

Benner, S. G., Polizzotto, M. L., Kocar, B. D., Ganguly, S., Phan, K., Ouch, K., ... Fendorf, S. (2008). Groundwater flow in an arsenic-contaminated aquifer, Mekong Delta, Cambodia. *Applied Geochemistry*, 23(11), 3072–3087. https://doi.org/10.1016/j.apgeochem.2008.06.013

Bethke, C. M., & Johnson, T. M. (2008). Groundwater age and groundwater age dating. *Annual Review of Earth and Planetary Sciences*, 36(1), 121–152. https://doi.org/10.1146/annurev.earth.36.031207.124210

Beven, K., & Binley, A. (1992). The future of distributed models: Model calibration and uncertainty prediction. *Hydrological Processes*, 6(3), 279–298. https://doi.org/10.1002/hyp.3360060305

Birkel, C., Dunn, S. M., Tetzlaff, D., & Soulsby, C. (2010). Assessing the value of high-resolution isotope tracer data in the stepwise development of a lumped conceptual rainfall–runoff model. *Hydrological Processes*, 24(16), 2335–2348. https://doi.org/10.1002/hyp.7763

Birkel, C., Geris, J., Molina, M. J., Mendez, C., Arce, R., Dick, J., ... Soulsby, C. (2016). Hydroclimatic controls on non-stationary stream water ages in humid tropical catchments. *Journal of Hydrology*, 542, 231–240. https://doi.org/10.1016/j.jhydrol.2016.09.006

Boehmer, W. (2000). Ground water study Mekong Delta. HASKONING B. V. Consulting Engineers and Architects, in association with Division of Hydro-Geology and Engineering Geology for the South of Vietnam and ARCADIS Euroconsult, 136.

Bonell, M., & Bruijnzeel, L. A. (2005). *Forests, water and people in the humid tropics: Past, present and future hydrological research for integrated land and water management*. New York: Cambridge University Press.

Buschmann, J., Berg, M., Stengel, C., Winkel, L, Sampson, M. L., Trang, P. T. K., & Viet, P. H. (2008). Contamination of drinking water resources in the Mekong Delta floodplains: Arsenic and other trace metals pose serious health risks to population. *Environment International*, 34(6), 756–764. https://doi.org/10.1016/j.envint.2007.12.025

Calderon, H., & Uhlenbrook, S. (2016). Characterizing the climatic water balance dynamics and different runoff components in a poorly gauged tropical forested catchment, Nicaragua. *Hydrological Sciences Journal*, 61(14), 2465–2480. https://doi.org/10.1080/02626667.2014.964244

Cartwright, I., & Morgenstern, U. (2016). Contrasting transit times of water from peatlands and eucalypt forests in the Australian Alps determined by tritium: Implications for vulnerability and the source of water in upland catchments. *Hydrology and Earth System Sciences*, 20(12), 4757–4773. https://doi.org/10.5194/hess-20-4757-2016

Clark, I. D., & Fritz, P. (1997). *Environmental isotopes in hydrogeology*. New York: CRC Press.

Cook, P. G., & Böhlke, J.-K. (2000). *Determining timescales for groundwater flow and solute transport Environmental tracers in subsurface hydrology* (pp. 1–30). New York: Springer.

Danh, V. T., & Khai, H. V. (2015). Household demand and supply for clean groundwater in the Mekong Delta, Vietnam. *Renewables: Wind, Water, and Solar*, 2(1), 4. https://doi.org/10.1186/s40807-014-0004-7

Darling, W., Morris, B., Stuart, M., & Gooddy, D. (2005). Groundwater age indicators from public supplies tapping the Chalk aquifer of Southern England. *Water Environment Journal*, 19(1), 30–40. https://doi.org/10.1111/j.1747-6593.2005.tb00546.x

Dunn, S. M., Bacon, J. R., Soulsby, C., Tetzlaff, D., Stutter, M. I., Waldron, S., & Malcolm, I. A. (2008). Interpretation of homogeneity in δ18O signatures of stream water in a nested sub-catchment system in north-east Scotland. *Hydrological Processes*, 22(24), 4767–4782. https://doi.org/10.1002/hyp.7088

Duvert, C., Stewart, M., Cendón, D., & Raiber, M. (2016). Time series of tritium, stable isotopes and chloride reveal short-term variations in groundwater contribution to a stream. *Hydrology and Earth System Sciences*, 20(1), 257–277. https://doi.org/10.5194/hess-20-257-2016

Duy, N. L., Heidbüchel, I., Meyer, H., Merz, B., & Apel, H. (2018). What controls the stable isotope composition of precipitation in the Mekong Delta? A model-based statistical approach. *Hydrology and Earth System Sciences*, 22(2), 1239–1262. https://doi.org/10.5194/hess-22-1239-2018

Eberts, S. M., Böhlke, J. K., Kauffman, L. J., & Jurgens, B. C. (2012). Comparison of particle-tracking and lumped-parameter age-distribution models for evaluating vulnerability of production wells to contamination. *Hydrogeology Journal*, 20(2), 263–282. https://doi.org/10.1007/s10040-011-0810-6

Erban, L. E., Gorelick, S. M., Zebker, H. A., & Fendorf, S. (2013). Release of arsenic to deep groundwater in the Mekong Delta, Vietnam, linked to pumping-induced land subsidence. *Proceedings of the National Academy of Sciences*, 110(34), 13751–13756. https://doi.org/10.1073/pnas.1300503110

Farrick, K. K., & Branfireun, B. A. (2015). Flowpaths, source water contributions and water residence times in a Mexican tropical dry forest catchment. *Journal of Hydrology*, 529, 854–865. https://doi.org/10.1016/j.jhydrol.2015.08.059

Fetter, C. (2001). *Applied hydrogeology* (4th ed.) (p. 598). Upper Saddle River, NJ: Prentice Hall.

Grabczak, J., Różański, K., Maloszewski, P., & Zuber, A. (1984). Estimation of the tritium input function with the aid of stable isotopes. *Catena*, 11(2), 105–114. https://doi.org/10.1016/0341-8162(84)90001-8

GSO (2016). *Statistical yearbook of Vietnam 2016*. Hanoi: General Statistics Office (GSO) Vietnam.

Gupta, H. V., Kling, H., Yilmaz, K. K., & Martinez, G. F. (2009). Decomposition of the mean squared error and NSE performance criteria: Implications for improving hydrological modelling. *Journal of Hydrology*, 377(1), 80–91. https://doi.org/10.1016/j.jhydrol.2009.08.003

Heidbüchel, I., Troch, P. A., Lyon, S. W., & Weiler, M. (2012). The master transit time distribution of variable flow systems. *Water Resources Research*, 48(6). https://doi.org/10.1029/2011WR011293

Hiscock, K. M., & Grischek, T. (2002). Attenuation of groundwater pollution by bank filtration. *Journal of Hydrology*, 266(3), 139–144. https://doi.org/10.1016/S0022-1694(02)00158-0

Ho, H. D., Aramyossy, J., Louvat, D., Huu, M., Nguyen, T. V., & Nguyen, K. C. (1991). *Environmental isotope study related to the origin, salinization and movement of groundwater in the Mekong Delta (Viet Nam)* (pp. 415–428). Isotopes techniques in Water Resource Development.

Hoang, T. H., Bang, S., Kim, K.-W., Nguyen, M. H., & Dang, D. M. (2010). Arsenic in groundwater and sediment in the Mekong river delta, Vietnam. *Environmental Pollution*, 158(8), 2648–2658. https://doi.org/10.1016/j.envpol.2010.05.001

Hrachowitz, M., Savenije, H., Bogaard, T. A., Tetzlaff, D., & Soulsby, C. (2013). What can flux tracking teach us about water age distribution patterns and their temporal dynamics? *Hydrology and Earth System Sciences*, 17(2), 533–564. https://doi.org/10.5194/hess-17-533-2013

Hrachowitz, M., Soulsby, C., Tetzlaff, D., Dawson, J. J. C., Dunn, S. M., & Malcolm, I. A. (2009). Using long-term data sets to understand transit times in contrasting headwater catchments. *Journal of Hydrology*, 367(3), 237–248. https://doi.org/10.1016/j.jhydrol.2009.01.001

Hrachowitz, M., Soulsby, C., Tetzlaff, D., & Malcolm, I. A. (2011). Sensitivity of mean transit time estimates to model conditioning and data availability. *Hydrological Processes*, 25(6), 980–990. https://doi.org/10.1002/hyp.7922

Hrachowitz, M., Soulsby, C., Tetzlaff, D., Malcolm, I. A., & Schoups, G. (2010). Gamma distribution models for transit time estimation in catchments: Physical interpretation of parameters and implications for time-variant transit time assessment. *Water Resources Research*, 46(10), n/a–n/a. https://doi.org/10.1029/2010WR009148

Jacobs, S. R., Timbe, E., Weeser, B., Rufino, M. C., Butterbach-Bahl, K., & Breuer, L. (2018). Assessment of hydrological pathways in East African montane catchments under different land use. *Hydrology and Earth System Sciences*, 22(9), 4981–5000. https://doi.org/10.5194/hess-22-4981-2018

Johnston, R., & Kummu, M. (2012). Water resource models in the Mekong basin: A review. *Water Resources Management*, 26(2), 429–455. https://doi.org/10.1007/s11269-011-9925-8

Kabeya, N., Katsuyama, M., Kawasaki, M., Ohte, N., & Sugimoto, A. (2007). Estimation of mean residence times of subsurface waters using seasonal variation in deuterium excess in a small headwater catchment in Japan. *Hydrological Processes*, 21(3), 308–322. https://doi.org/10.1002/hyp.6231

Kármán, K., Maloszewski, P., Deák, J., Fórizs, I., & Szabó, C. (2014). Transit time determination for a riverbank filtration system using oxygen isotope data and the lumped-parameter model. *Hydrological Sciences Journal*, 59(6), 1109–1116. https://doi.org/10.1080/02626667.2013.808345

Kazama, S., Hagiwara, T., Ranjan, P., & Sawamoto, M. (2007). Evaluation of groundwater resources in wide inundation areas of the Mekong river basin. *Journal of Hydrology*, 340(3), 233–243. https://doi.org/10.1016/j.jhydrol.2007.04.017

Kirchner, J. W. (2016a). Aggregation in environmental systems—Part 1: Seasonal tracer cycles quantify young water fractions, but not mean transit times, in spatially heterogeneous catchments. *Hydrology and Earth System Sciences*, 20(1), 279–297. https://doi.org/10.5194/hess-20-279-2016

Kirchner, J. W. (2016b). Aggregation in environmental systems—Part 1: Seasonal tracer cycles quantify young water fractions, but not mean transit times, in spatially heterogeneous catchments. *Hydrology and Earth System Sciences*, 20(1), 279–297. https://doi.org/10.5194/hess-20-279-2016

Kirchner, J. W., Feng, X., & Neal, C. (2000). Fractal stream chemistry and its implications for contaminant transport in catchments. *Nature*, 403(6769), 524–527. https://doi.org/10.1038/35000537

Kocar, B. D., Polizzotto, M. L., Benner, S. G., Ying, S. C., Ung, M., Ouch, K., … Fendorf, S. (2008). Integrated biogeochemical and hydrologic processes driving arsenic release from shallow sediments to groundwaters of the Mekong Delta. *Applied Geochemistry*, 23(11), 3059–3071. https://doi.org/10.1016/j.apgeochem.2008.06.026

Koeniger, P., Gaj, M., Beyer, M., & Himmelsbach, T. (2016). Review on soil water isotope-based groundwater recharge estimations. *Hydrological Processes*, 30(16), 2817–2834. https://doi.org/10.1002/hyp.10775

Lamontagne, S., Taylor, A., Batlle-Aguilar, J., Suckow, A., Cook, P., Smith, S., … Stewart, M. (2015). River infiltration to a subtropical alluvial aquifer inferred using multiple environmental tracers. *Water Resources Research*, 51(6), 4532–4549. https://doi.org/10.1002/2014WR015663

Lawson, M., Polya, D. A., Boyce, A. J., Bryant, C., & Ballentine, C. J. (2016). Tracing organic matter composition and distribution and its role on arsenic release in shallow Cambodian groundwaters. *Geochimica et Cosmochimica Acta*, 178, 160–177. https://doi.org/10.1016/j.gca.2016.01.010

Lawson, M., Polya, D. A., Boyce, A. J., Bryant, C., Mondal, D., Shantz, A., & Ballentine, C. J. (2013). Pond-derived organic carbon driving changes in arsenic hazard found in Asian groundwaters. *Environmental Science & Technology*, 47(13), 7085–7094. https://doi.org/10.1021/es400114q

Le Luu, T. (2017). Remarks on the current quality of groundwater in Vietnam. *Environmental Science and Pollution Research*, 26, 1163–1169. https://doi.org/10.1007/s11356-017-9631-z

Leibundgut, C., Maloszewski, P., & Külls, C. (2011). *Tracers in hydrology*. Chichester: John Wiley & Sons.

Maloszewski, P. (2000). *Lumped-parameter models as a tool for determining the hydrological parameters of some groundwater systems based on isotope data* (Vol. 262) (pp. 271–276). IAHS Publication (International Association of Hydrological Sciences).

Maloszewski, P., Rauert, W., Trimborn, P., Herrmann, A., & Rau, R. (1992). Isotope hydrological study of mean transit times in an alpine basin (Wimbachtal, Germany). *Journal of Hydrology*, 140(1), 343–360. https://doi.org/10.1016/0022-1694(92)90247-S

Maloszewski, P., Stichler, W., Zuber, A., & Rank, D. (2002). Identifying the flow systems in a karstic-fissured-porous aquifer, the Schneealpe, Austria, by modelling of environmental ^{18}O and ^{3}H isotopes. *Journal of Hydrology*, 256(1), 48–59. https://doi.org/10.1016/S0022-1694(01)00526-1

Małoszewski, P., & Zuber, A. (1982). Determining the turnover time of groundwater systems with the aid of environmental tracers: 1. Models and their applicability. *Journal of Hydrology*, 57(3), 207–231. https://doi.org/10.1016/0022-1694(82)90147-0

Maloszewski, P., & Zuber, A. (1996). Lumped parameter models for the interpretation of environmental tracer data. *International Atomic Energy Agency*, 28(6), 9–58.

McGuire, K., DeWalle, D., & Gburek, W. (2002). Evaluation of mean residence time in subsurface waters using oxygen-18 fluctuations during drought conditions in the mid-Appalachians. *Journal of Hydrology*, 261(1), 132–149. https://doi.org/10.1016/S0022-1694(02)00006-9

McGuire, K. J., & McDonnell, J. J. (2006). A review and evaluation of catchment transit time modeling. *Journal of Hydrology*, 330(3), 543–563. https://doi.org/10.1016/j.jhydrol.2006.04.020

Merola, R. B., Hien, T. T., Quyen, D. T. T., & Vengosh, A. (2015). Arsenic exposure to drinking water in the Mekong Delta. *Science of the Total Environment*, 511, 544–552. https://doi.org/10.1016/j.scitotenv.2014.12.091

Meyer, H., Schönicke, L., Wand, U., Hubberten, H.-W., & Friedrichsen, H. (2000). Isotope studies of hydrogen and oxygen in ground ice-experiences with the equilibration technique. *Isotopes in Environmental and Health Studies*, 36(2), 133–149. https://doi.org/10.1080/10256010008032939

Minderhoud, P., Erkens, G., Pham, V., Bui, V. T., Erban, L., Kooi, H., & Stouthamer, E. (2017). Impacts of 25 years of groundwater extraction on subsidence in the Mekong Delta, Vietnam. *Environmental Research Letters*, 12(6), 064006. https://doi.org/10.1088/1748-9326/aa7146

Mook, W., & Rozanski, K. (2000). *Environmental isotopes in the hydrological cycle* (Vol. 39). Vienna: IAEA Publish.

Morgenstern, U., Daughney, C. J., Leonard, G., Gordon, D., Donath, F. M., & Reeves, R. (2015). Using groundwater age and hydrochemistry to understand sources and dynamics of nutrient contamination through the catchment into Lake Rotorua, New Zealand. *Hydrology and Earth System Sciences*, 19(2), 803–822. https://doi.org/10.5194/hess-19-803-2015

Mosquera, G. M., Segura, C., Vaché, K. B., Windhorst, D., Breuer, L., & Crespo, P. (2016). Insights into the water mean transit time in a high-elevation tropical ecosystem. *Hydrology and Earth System Sciences*, 20(7), 2987–3004. https://doi.org/10.5194/hess-20-2987-2016

Muñoz-Villers, L. E., Geissert, D. R., Holwerda, F., & McDonnell, J. J. (2016). Factors influencing stream baseflow transit times in tropical montane watersheds. *Hydrology and Earth System Sciences*, 20(4), 1621–1635. https://doi.org/10.5194/hess-20-1621-2016

Muñoz-Villers, L. E., & McDonnell, J. J. (2012). Runoff generation in a steep, tropical montane cloud forest catchment on permeable volcanic substrate. *Water Resources Research*, 48(9). https://doi.org/10.1029/2011WR011316

Nam, N. D. G., Goto, A., & Osawa, K. (2017). Groundwater modeling for groundwater management in the coastal area of Mekong Delta, Vietnam. *Transactions of The Japanese Society of Irrigation, Drainage and Rural Engineering*, 85(1), I_93–I_103.

Nguyen, V. L., Ta, T. K. O., & Tateishi, M. (2000). Late Holocene depositional environments and coastal evolution of the Mekong river delta, Southern Vietnam. *Journal of Asian Earth Sciences*, 18(4), 427–439. https://doi.org/10.1016/S1367-9120(99)00076-0

Nuber, T., Van Nam, V., & Stolpe, H. (2009). VI-4: Modelling the groundwater dynamics of Can Tho City—Challenges, approaches, solutions. In *Closing Nutrient Cycles in Decentralised Water Treatment Systems in the Mekong Delta* (p. 236). Tokyo, Japan: The Japanese Society of Irrigation, Drainage and Rural Engineering.

Raksmey, M., Jinno, K., & Tsutsumi, A. (2009). Effects of river water on groundwater in Cambodia. *Memoirs of the Faculty of Engineering, Kyushu University*, 69(3), 95–115.

Renaud, F. G., & Kuenzer, C. (2012). *The Mekong Delta system: Interdisciplinary analyses of a river delta*. Dordrecht, the Netherlands: Springer Environmental Science and Engineering.

Richards, L. A., Magnone, D., Boyce, A. J., Casanueva-Marenco, M. J., van Dongen, B. E., Ballentine, C. J., & Polya, D. A. (2018). Delineating sources of groundwater recharge in an arsenic-affected Holocene aquifer in Cambodia using stable isotope-based mixing models. *Journal of Hydrology*, 557, 321–334. https://doi.org/10.1016/j.jhydrol.2017.12.012

Rinaldo, A., Beven, K. J., Bertuzzo, E., Nicotina, L., Davies, J., Fiori, A., … Botter, G. (2011). Catchment travel time distributions and water flow in soils. *Water Resources Research*, 47(7). https://doi.org/10.1029/2011WR010478

Roa-García, M. C., & Weiler, M. (2010). Integrated response and transit time distributions of watersheds by combining hydrograph separation and long-term transit time modeling. *Hydrology and Earth System Sciences*, 14(8), 1537–1549. https://doi.org/10.5194/hess-14-1537-2010

Seeger, S., & Weiler, M. (2014). Reevaluation of transit time distributions, mean transit times and their relation to catchment topography. *Hydrology and Earth System Sciences*, 18(12), 4751–4771. https://doi.org/10.5194/hess-18-4751-2014

Shinkai, Y., Truc, D. V., Sumi, D., Canh, D., & Kumagai, Y. (2007). Arsenic and other metal contamination of groundwater in the Mekong river delta, Vietnam. *Journal of Health Science*, 53(3), 344–346. https://doi.org/10.1248/jhs.53.344

Skrzypek, G., Mydłowski, A., Dogramaci, S., Hedley, P., Gibson, J. J., & Grierson, P. F. (2015). Estimation of evaporative loss based on the stable isotope composition of water using hydrocalculator. *Journal of Hydrology*, *523*, 781–789. https://doi.org/10.1016/j.jhydrol.2015.02.010

Stanger, G., Truong, T. V., Ngoc, K. S. L. T. M., Luyen, T. V., & Thanh, T. T. (2005). Arsenic in groundwaters of the Lower Mekong. *Environmental Geochemistry and Health*, *27*(4), 341–357. https://doi.org/10.1007/s10653-005-3991-x

Stewart, M., Morgenstern, U., McDonnell, J., & Pfister, L. (2012). The 'hidden streamflow' challenge in catchment hydrology: A call to action for stream water transit time analysis. *Hydrological Processes*, *26*(13), 2061–2066. https://doi.org/10.1002/hyp.9262

Stewart, M., & Thomas, J. (2008). A conceptual model of flow to the Waikoropupu Springs, NW Nelson, New Zealand, based on hydrometric and tracer (18 O, Cl, 3 H and CFC) evidence. *Hydrology and Earth System Sciences Discussions*, *12*(1), 1–19. https://doi.org/10.5194/hess-12-1-2008

Stewart, M. K., & McDonnell, J. J. (1991). Modeling base flow soil water residence times from deuterium concentrations. *Water Resources Research*, *27*(10), 2681–2693. https://doi.org/10.1029/91WR01569

Stewart, M. K., Mehlhorn, J., & Elliott, S. (2007). Hydrometric and natural tracer (oxygen-18, silica, tritium and sulphur hexafluoride) evidence for a dominant groundwater contribution to Pukemanga Stream, New Zealand. *Hydrological Processes*, *21*(24), 3340–3356. https://doi.org/10.1002/hyp.6557

Stewart, M. K., Morgenstern, U., Gusyev, M. A., & Małoszewski, P. (2017). Aggregation effects on tritium-based mean transit times and young water fractions in spatially heterogeneous catchments and groundwater systems. *Hydrology and Earth System Sciences*, *21*(9), 4615–4627. https://doi.org/10.5194/hess-21-4615-2017

Stewart, M. K., Morgenstern, U., & McDonnell, J. J. (2010). Truncation of stream residence time: How the use of stable isotopes has skewed our concept of streamwater age and origin. *Hydrological Processes*, *24*(12), 1646–1659. https://doi.org/10.1002/hyp.7576

Stichler, W., Maloszewski, P., Bertleff, B., & Watzel, R. (2008). Use of environmental isotopes to define the capture zone of a drinking water supply situated near a dredge lake. *Journal of Hydrology*, *362*(3), 220–233. https://doi.org/10.1016/j.jhydrol.2008.08.024

Stichler, W., Maloszewski, P., & Moser, H. (1986). Modelling of river water infiltration using oxygen-18 data. *Journal of Hydrology*, *83*(3-4), 355–365. https://doi.org/10.1016/0022-1694(86)90161-7

Stockinger, M. P., Bogena, H. R., Lücke, A., Diekkrüger, B., Weiler, M., & Vereecken, H. (2014). Seasonal soil moisture patterns: Controlling transit time distributions in a forested headwater catchment. *Water Resources Research*, *50*(6), 5270–5289. https://doi.org/10.1002/2013WR014815

Stumpp, C., Stichler, W., & Maloszewski, P. (2009). Application of the environmental isotope δ^{18}O to study water flow in unsaturated soils planted with different crops: Case study of a weighable lysimeter from the research field in Neuherberg, Germany. *Journal of Hydrology*, *368*(1), 68–78. https://doi.org/10.1016/j.jhydrol.2009.01.027

Tetzlaff, D., Birkel, C., Dick, J., Geris, J., & Soulsby, C. (2014). Storage dynamics in hydropedological units control hillslope connectivity, runoff generation, and the evolution of catchment transit time distributions. *Water Resources Research*, *50*(2), 969–985. https://doi.org/10.1002/2013WR014147

Thiemig, V., Rojas, R., Zambrano-Bigiarini, M., & De Roo, A. (2013). Hydrological evaluation of satellite-based rainfall estimates over the Volta and Baro-Akobo Basin. *Journal of Hydrology*, *499*, 324–338. https://doi.org/10.1016/j.jhydrol.2013.07.012

Thu, N. T. (2017). Groundwater and surface water cycle system in Mekong Delta, Vietnam. 171. doi:https://tsukuba.repo.nii.ac.jp/?action=repository_uri&item_id=43117&file_id=17&file_no=1

Timbe, E., Windhorst, D., Celleri, R., Timbe, L., Crespo, P., Frede, H. G., … Breuer, L. (2015). Sampling frequency trade-offs in the assessment of mean transit times of tropical montane catchment waters under semi-steady-state conditions. *Hydrology and Earth System Sciences*, *19*(3), 1153–1168. https://doi.org/10.5194/hess-19-1153-2015

Timbe, E., Windhorst, D., Crespo, P., Frede, H. G., Feyen, J., & Breuer, L. (2014). Understanding uncertainties when inferring mean transit times of water trough tracer-based lumped-parameter models in Andean tropical montane cloud forest catchments. *Hydrology and Earth System Sciences*, *18*(4), 1503–1523. https://doi.org/10.5194/hess-18-1503-2014

Vermeulen, P., Quan, N. H., Nam, N. D. G., Hung, P. V., Tung, N., Thanh, T., & Rien, D. (2013). Groundwater modeling for the Mekong Delta using iMOD. In *Paper presented at the MODSIM2013, 20th International Congress on Modelling and Simulation*. Zealand: Modelling and Simulation Society of Australia and New.

Viville, D., Ladouche, B., & Bariac, T. (2006). Isotope hydrological study of mean transit time in the granitic Strengbach catchment (Vosges massif, France): Application of the FlowPC model with modified input function. *Hydrological Processes: An International Journal*, *20*(8), 1737–1751. https://doi.org/10.1002/hyp.5950

Wagner, F., Tran, V. B., & Renaud, F. G. (2012). *Groundwater resources in the Mekong Delta: Availability, utilization and risks The Mekong Delta System* (pp. 201–220). Dordrecht, the Netherlands: Springer.

Weiler, M., McGlynn, B. L., McGuire, K. J., & McDonnell, J. J. (2003). How does rainfall become runoff? A combined tracer and runoff transfer function approach. *Water Resources Research*, *39*(11), n/a–n/a. https://doi.org/10.1029/2003WR002331

Wentworth, C. K. (1922). A scale of grade and class terms for clastic sediments. *The Journal of Geology*, *30*(5), 377–392. https://doi.org/10.1086/622910

Wilbers, G.-J., Sebesvari, Z., & Renaud, F. (2014). Piped-water supplies in rural areas of the Mekong Delta, Vietnam: Water quality and household perceptions. *Water*, *6*(8), 2175–2194. https://doi.org/10.3390/w6082175

Zuber, A., Różański, K., Kania, J., & Purtschert, R. (2011). On some methodological problems in the use of environmental tracers to estimate hydrogeologic parameters and to calibrate flow and transport models. *Hydrogeology Journal*, *19*(1), 53–69. https://doi.org/10.1007/s10040-010-0655-4

SUPPORTING INFORMATION

Additional supporting information may be found online in the Supporting Information section at the end of this article.